J. Fluid Mech. (1980), *vol.* 90, *part.* 4, *pp.* 727–753
Printed in Great Britain

On the severe non-symmetric constriction, curving or cornering of channel flows

By F. T. SMITH
Applied Mathematics Department, University of Western Ontario, London, Ontario, Canada†

AND P. W. DUCK
Department of Aeronautical and Astronautical Engineering, Ohio State University, Columbus, Ohio 43210, U.S.A.‡

(Received 17 July 1979)

Considered below is the plane, high-Reynolds-number (Re), flow of an incompressible fluid through a channel suffering a severe non-symmetric constriction, 'severe' meaning 'of typical dimensions comparable with the channel width a^*'. The (mainly inviscid) flow description is governed by free streamline theory, to be consistent with the viscous incompressible separation from the constriction surface and with a relatively slow eddy motion beyond. Separation also occurs far ahead of the constriction, at a distance $O(Re^{\frac{1}{7}} a^*)$ upstream. Attention is given primarily to the flow features for a particular class of slowly varying severe constrictions, from which however the features for the probably more useful classes of slender (i.e. of large length but $O(a^*)$ height) and moderately severe (i.e. of $O(a^*)$ length but small height) constriction follow, as do those for curved or cornered channel flows. In all these cases a long-scale flow response is induced upstream and downstream and in many cases remarkably simple universal formulae for the separation and reattachment positions result. The corresponding $O(a^*)$ corrections to the upstream separation distance above are also derived.

1. Introduction

In the field of internal streaming flows there are a great many fundamental, but challenging, theoretical problems. Some clear understanding of such problems seems necessary before the more practical internal flow problems most directly associated with physiology and engineering may be tackled with any degree of accuracy or theoretical certainty. Even for the most basic cases of steady laminar flow of an incompressible Newtonian fluid through a plane channel or an axisymmetric pipe, with fixed walls, the variety of problems introduced purely by the different geometrical arrangements possible (involving, for example, constriction, dilation, curvature, cornering, branching, blockaging, junctions, or combinations thereof) is such that at first sight our present analytical knowledge may seem rather limited in contrast. The apparent contrast becomes still more stark when one also brings into theoretical consideration the added effects of unsteadiness, three-dimensionality, compressibility,

† Permanent address: Mathematics Department, Imperial College, London SW7, U.K.
‡ Permanent address: Mathematics Department, The University, Manchester, U.K.

non-Newtonian properties, non-rigid walls, stability, or, sometimes most importantly, turbulence.

On the other hand the fact that separation, which is almost inevitably found at moderate or high Reynolds numbers in any of the above flow situations, has only been treatable theoretically in the last decade or so, following Stewartson & Williams' (1969) explanation of external supersonic flow separation, perhaps accounts largely for this discrepancy in analytical understanding. Certainly, since 1969 a good deal of analytical progress has been possible in studies of both internal and external flows at high Reynolds numbers. The main idea stemming from Stewartson & Williams' (1969) work (see also Messiter 1970) is that separation usually occurs by means of a free interaction, a local, fairly abrupt, viscous-inviscid process. This idea has proved extremely fruitful in studies of supersonic and subsonic external motions (see the reviews by Stewartson 1974 and Messiter 1979) and, of more concern to the present paper, in studies of internal, channel or pipe flows also (Smith 1976*a–c*, 1977*a*, 1979*a*). A characteristic property predicted in the latter studies, for symmetric flow situations at least, is the occurrence of separation both far upstream and near a point of maximum constriction at high Reynolds numbers, if the internal flow suffers a substantial disturbance; some, but by no means all, of the evidence from numerical solutions of the Navier–Stokes equations and from experimental measurements is in line with that prediction. A review of the internal flow studies is given by Smith (1979*a*) and so for our present interest, in non-symmetric channel flows at high Reynolds numbers, we need describe only the basics of Smith's (1977*a*) work on such channel flows.

The conclusion of Smith (1977*a*) is that, far ahead of any severe non-symmetric disturbance to an oncoming plane Poiseuille flow, at high Reynolds numbers, a nonlinear free interaction must take place on a large length scale of order $a^* Re^{\frac{1}{7}}$, where $Re(\gg 1)$ is the Reynolds number (see § 2 below) based on the undisturbed channel width a^*. Here 'severe' means 'of characteristic dimensions comparable with a^*' if the disturbance is a distortion of the wall, or 'finite' in general. One minor reservation needs to be made to the above conclusion, incidentally: if the severe non-symmetric disturbance is such that the original plane Poiseuille flow itself forms an acceptable first inviscid approximation, at $O(a^*)$ distances from the disturbance, then the nonlinear free interaction upstream is unlikely to occur. An example of such a disturbance is a severe dilatation of the channel, where the Poiseuille flow can sweep almost unaltered past the dilatation and leave only a relatively slow-moving eddy of recirculating fluid adjoining the dilatation. For a severe non-symmetric constriction, however, where the Poiseuille flow is clearly not an acceptable first approximation, the upstream free interaction and the flow separation associated with it have the effect of adjusting the oncoming flow nonlinearly before the actual constriction is reached. The local flow near the constriction then has to merge upstream with the algebraic terminal form (given in §§ 5, 6 of Smith 1977*a*) of the free interaction, rather than with the initial, exponential, form of deviation (§ 3 of Smith 1977*a*) from the Poiseuille flow at the start of the free interaction. Further, the free interaction leads to the prediction

$$0{\cdot}49a^*[2(30q)^3 Re]^{\frac{1}{7}} - Da^*, \tag{1.1}$$

for the distance between the constriction and the upstream separation point, where q is an $O(1)$ constant depending on the oncoming velocity profile [see after (2.3) below; $q = \frac{1}{30}$ for Poiseuille flow] and the $O(1)$ constant D is to be determined. Comparisons between the leading term in (1.1) and numerical solutions of the Navier–Stokes equations for increasingly high Reynolds numbers have already shown encouraging agreement (Smith 1977*a*), as have similar comparisons for symmetrically constricted pipe and channel flows (Smith 1979*a*; Dennis & Smith 1980).

Our aim in this paper is to provide a complete theoretical account of the high-Reynolds-number motion through a severe non-symmetric constriction and in particular to determine the value of D in (1.1), for a given constriction shape, and the positions of the reattachment(s) and separation(s) which must take place subsequently. The work is restricted to steady laminar plane flow of an incompressible Newtonian fluid and is based on free streamline theory, of the Kirchhoff (1869) kind, in order to be consistent with, first, the viscous separations occurring (for a smooth bounded constriction) both upstream of and on the constriction and, secondly, the presence of only slowly moving eddies between any free streamline and the wall from which that free streamline detaches at separation. Here the upstream separation is that associated with the free interaction leading to (1.1), while the separation on the constriction is described by the Sychev (1972)–Smith (1977*b*) triple-deck. Also the postulate of slowly moving eddies is almost certainly consistent with the flow properties at the reattachments involved. For (as in Smith 1979*a*) the first reattachment, an inviscid process near the constriction surface, provokes only small reversed velocities; and the second reattachment takes place at such a large distance ($O(a^*Re)$) downstream that viscous forces are able to prevent any significant backflow being promoted. Both reattachments are somewhat different from those occurring in the corresponding, bluff body, external flow situation (Smith 1979*b*), therefore.

The free streamline flow features are summarized in § 2 below; some of the properties of symmetrically constricted flows (Smith 1979*a*) carry over to our non-symmetric case, allowing some curtailment of the discussion of § 2, but one vital difference is the algebraic decay upstream, referred to previously. Many other significant differences then arise when solutions for the free streamline flow are sought (§§ 3–6). First § 3 investigates a rather bizarre-looking class, of slowly varying severe constrictions of streamwise length scale $O(al)$ and transverse height scale $O(al^{-2})$ where $l \gg 1$. However, the long-scale theory for this slowly varying class provides the key to the flow properties for the probably more realistic classes of slender constrictions (those of length $\gg a^*$ but height of $O(a^*)$) and moderately severe constrictions (those of length $O(a^*)$ but height $ha^* \ll a^*$) considered next in § 4. In particular, the moderately severe class induces perturbations (of relative orders h and $h^{\frac{3}{2}}$) to the oncoming flow that are much greater than those (of relative order h^2 only) induced in the corresponding symmetrically constricted motions (Smith 1979*a*) and the flow structure then is a much more subtle affair, involving the length $h^{-\frac{1}{2}}a^*$ on which the constriction appears as a normal flat plate and the pressure variation across the channel still exerts a significant effect (§ 4.2). The long-scale theory applies also to the two other classical flows studied in §§ 5, 6, concerning curved and cornered channels respectively. The theory of §§ 2–6 deals with a general oncoming flow whose main, streamwise, velocity profile satisfies the no slip constraint at the channel walls; plane Poiseuille flow is one special case. Further comments are made in § 7.

2. General features of severely distorted channel flows

Letting a^*, U_∞^*, ν^*, ρ^* denote the undistorted channel width, a typical velocity of the oncoming flow, and the kinematic viscosity and density of the (incompressible) fluid, respectively, we define the Reynolds number to be $Re \equiv U_\infty^* a^*/\nu^*$ and use the velocities u, v, the corresponding Cartesian co-ordinates x, y (see figure 1) and the pressure p, non-dimensionalized with respect to U_∞^*, U_∞^*, a^*, a^*, $\rho^* U_\infty^{*2}$ in turn. The oncoming flow is taken to be essentially a velocity profile $u = U_0(y)$, but $|v| \ll 1$, such that $U_0(0) = U_0(1) = 0$, $U_0(y) > 0$ for $0 < y < 1$ and, for convenience, $U_0(y)$ is symmetric about $y = \frac{1}{2}$ with $U_0'(0) = 1$. For an oncoming Poiseuillean flow, for example, $U_0(y) = (y - y^2)$, $v = 0$.

To be definite in this section, we consider the fluid motion when only one of the channel walls (that originally at $y = 0$, say) is severely indented, giving a shape $y = F(x)$ for the lower wall but $y = 1$ for the upper wall, with $F(\pm\infty) = 0$, $0 \leqslant F(x) < 1$, and $F(x)$ is generally of $O(1)$. The modifications to the theory for other forms of constriction, or for cornered or curved channels, are readily made (see §§ 3–6 below).

When $Re \gg 1$ the flow field through the severely distorted channel is similar in some respects to the symmetric case of Smith (1979*a*) and is described by the expansions

$$(u, v, p) = (U, V, P) + O(Re^{-\frac{1}{16}}) \tag{2.1}$$

for x, y of $O(1)$. Here U, V, P satisfy the nonlinear inviscid equations of motion

$$\left.\begin{aligned} U_x + V_y &= 0, \\ UU_x + VU_y &= -P_x, \\ UV_x + VV_y &= -P_y. \end{aligned}\right\} \tag{2.2a}$$

These can be manipulated into the vorticity equation $\nabla^2\psi = \zeta(\psi)$, where $\psi(x, y)$ is the stream function ($U = \psi_y$, $V = -\psi_x$, $\psi(-\infty, 0) = 0$) and the unknown function ζ may be determined from the oncoming flow properties, via (2.5) below; but (2.2*a*) will suffice for most of our purposes. The boundary conditions to be imposed on (2.2*a*) are those appropriate to free streamline theory, analogous to the Kirchhoff (1869) kind with smooth separation from the indentation if the indentation shape $F(x)$ is smooth (cf. § 3.3 below), as in Smith (1979*a*). Thus on solid surfaces no adverse pressure gradients are tolerable, while on free streamlines the pressure must be uniform:

$$P = \text{constant}, \quad \psi = 0 \quad \text{on} \quad C_0C_1 \text{ and } C_2C_3; \tag{2.2b}$$

$$P_x < 0, \quad \psi = 0 \quad \text{on} \quad C_2C_3; \tag{2.2c}$$

$$P_x < 0, \quad \psi = \psi(-\infty, 1) \quad \text{on} \quad y = 1. \tag{2.2d}$$

Here the positions $x = x_1$, $x = x_2$ of C_1, C_2 (see figure 1) are unknown in advance. The conditions (2.2*c*, *d*) ensure consistent, attached, boundary-layer motions between the inviscid flow field of (2.2*a*) and the solid surfaces – it seems reasonable to look for a solution without separation along the upper wall, although if solutions of (2.2*a*) are not forthcoming then the question of separation there would need to be reconsidered – while (2.2*b*) is necessary for the eddying motions between the free streamlines (C_0C_1, C_2C_3) and the lower wall to remain relatively slow (with $U = V = 0$, $P =$ constant therein). Further, the smooth separation constraint above, at the position $x = x_2$ of figure 1, is required to ensure consistency between the inviscid breakaway of the free

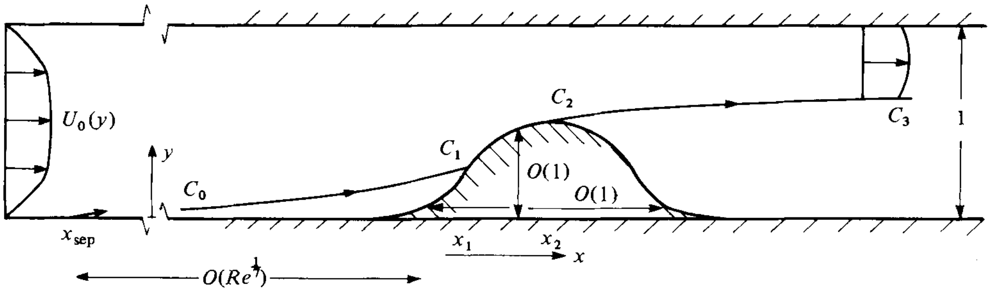

FIGURE 1. Schematic diagram of the severely constricted, non-symmetric, flow structure.

streamline from the solid surface and the viscous process of incompressible separation locally near $x = x_2$. The viscous process here has a triple-deck character (Smith 1979*b*) and demands that, as well as P being continuous,

$$P_x = 0 \quad \text{at} \quad x = x_2, \tag{2.2e}$$

whereas the $O(Re^{-\frac{1}{16}})$ correction in (2.1) has to exhibit a particular (inverse square root) form of singularity in pressure gradient at $x = x_2$. In general separation is expected to occur both upstream of, and on, the indentation, in order to avoid the adverse pressure gradients [accompanied by, e.g., the Goldstein (1948) singularity] that an attached-flow theory would otherwise predict unstream†, and towards the rear, of the indentation. In fact the upstream separation is governed by a free interaction and takes place asymptotically (and surprisingly) far ahead of the indentation, at a position $x = x_{sep}$ given by

$$x_{sep} = -0{\cdot}49(2[30q]^3 \,\mathrm{Re})^{\frac{1}{7}} + D, \tag{2.3}$$

from Smith's (1977*a*) work, where D (the origin shift) is an unknown constant dependent upon the solution of (2.2*a*–*e*), and $q = \int_0^1 U_0^2(y)\,dy$ ($= \frac{1}{30}$ for Poiseuille flow) is a given $O(1)$ parameter. This last work also yields the starting form for the unknown shape $y = F_1(x)$ of the free streamline upstream (figure 1), implying that

$$F_1(x) \sim 12q/(x-D)^2 \quad \text{for} \quad x \to -\infty\dagger \tag{2.4}$$

[see Smith 1977*a* equation (6.3*g*)].

One may verify that (2.4) is consistent with the solution of (2.2*a*–*e*) for $x \to -\infty$. Thus, writing $\psi_0'(y) = U_0(y)$ and

$$\left.\begin{aligned} \psi &= \psi_0(y) + (x-D)^{-2}\psi_1(y) + \dots, \\ P &= (x-D)^{-4} P_1(y) + \dots \end{aligned}\right\} \tag{2.5a}$$

for $x \to -\infty$ yields from (2.2*a*) and (2.2*b*)

$$\psi_1(y) = -A_1 U_0(y), \quad P_1(y) = -6A_1 \int_0^y U_0^2(y)\,dy \tag{2.5b}$$

† Clearly, at this stage we need to make the restriction that $F(x) \ll 12qx^{-2}$ as $x \to -\infty$; otherwise the indentation decays slowly enough upstream that the upstream separation of (2.4) is suppressed and attached-flow upstream is possible (cf. Smith 1979*a*, § 6).

(A_1 an unknown constant), following which Bernouilli's theorem applied along $y = 1$ yields

$$A_1 = 0 \quad \text{or} \quad A_1 = 12q. \tag{2.5c}$$

The former result for A_1 applies to non-distorted or symmetrically-distorted channel flows (only), while the latter reproduces (2.4), on imposing $\psi = 0$ at $y = F_1(x)$ with (2.5a, b). Our view is that the starting forms (2.3), (2.4), (2.5a–c), which are non-linear upstream eigensolutions in a sense, will arise for almost all non-symmetrically, severely, distorted channel flows. The results in §§3–6 below certainly add credence to such a view.

Despite the presence of the separating streamline far upstream, in (2.4), however, the upstream constraints,

$$\left.\begin{aligned} U(-\infty, y) = U_0(y), \psi(-\infty, y) = \psi_0(y), \\ P(-\infty, y) = 0, \end{aligned}\right\} \tag{2.6}$$

are still appropriate for $0 < y < 1$. Downstream, as in Smith (1979a), a boundedness condition is all that is necessary, and it leads to a separated jet-like flow persisting as $x \to \infty$; the ultimate reattachment of the last flow occurs on an x scale of $O(Re)$ downstream. At the first reattachment point $x = x_1$ the only smoothness conditions to be imposed are the obvious ones that P should be continuous and, by definition, $F_1(x_1 -) = F(x_1)$. A discontinuity in P_x or P_{xx} at C_1 is certainly permissible according to the present, somewhat limited, knowledge of reattachment processes.

The problem posed, (2.2a–e) with (2.6), sets a very difficult numerical task in general. Also, although the theory so far is quite similar in spirit to the symmetrical flow theory (Smith 1979a), significant differences are already apparent in the algebraic decay upstream in (2.4), (2.5a–c) and in the large upstream separation distance predicted in (2.3). Further distinctions arise when we move on to consider certain limit solutions of (2.2e), (2.6), namely slowly varying, slender and moderately severe constrictions, in §§3, 4 below.

3. Slowly-varying severe distortions

For an indentation whose typical length scale l is large, $l \gg 1$ (but, strictly, $l \ll Re^N$ for all $N > 0$ so that the Reynolds-number expansions of (2.1) remain undisturbed), it is found that some of the most important flow responses take place in thin wall layers of thickness $O(l^{-2})$. So we will study for the most part the properties of (2.2a–e), (2.6) for a particular class of slowly-varying indentations given by

$$y = l^{-2} f(X) \quad \text{where} \quad x = lX. \tag{3.1}$$

The flow features for many other classes of indentations, and for curved or cornered channels, stem directly from the properties resulting for the class (3.1), as §§4–6 show subsequently. We shall treat the general case of a smooth indentation (3.1) (with $f(\pm\infty) = 0$) in §3.1 below, and then §§3.2 and 3.3 deal with specific examples of smooth and non-smooth indentations.

3.1. *The long-scale theory*

For (3.1) the solution of (2.2a–e) with (2.6) subdivides into three basic zones, I–III when X is $O(1)$. Zone I is the core ($0 < y < 1$) of the motion, while II, III are wall

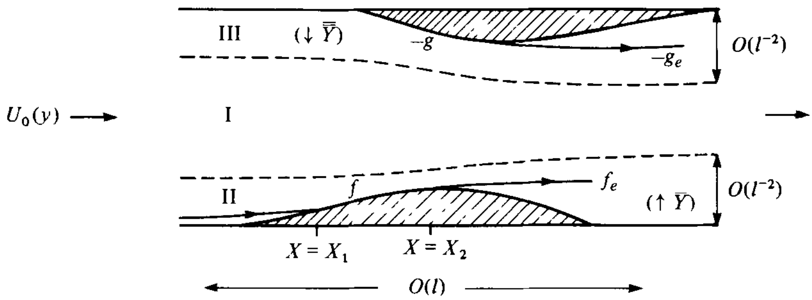

FIGURE 2. The flow structure for the slowly-varying severe constriction.

layers of thickness $O(l^{-2})$ astride $y = 0, 1$ respectively (see figure 2). In zone I the expansions for ψ, P are

$$\left.\begin{aligned} \psi &= \psi_0(y) + l^{-2}\psi_1(X, y) + O(l^{-3}), \\ P &= l^{-4}p_1(X, y) + O(l^{-5}), \end{aligned}\right\} \tag{3.2a}$$

and so (2.2*a*) yields the solutions

$$\psi_1 = A(X)\, U_0(y), \quad p_1 = P_1(X) + A''(X) \int_0^y U_0^2(\bar{y})\, d\bar{y}, \tag{3.2b}$$

where $P_1(X)$ is the unknown wall pressure at $y = 0$ and $A(X)$ is an unknown (displacement) function. Hence in zone II, to leading order,

$$\psi = l^{-4}\bar{\psi}(X, \bar{Y}), \quad P = l^{-4}P_1(X) \tag{3.3a}$$

with $y = l^{-2}\bar{Y}$, $\bar{Y} = O(1)$, and from (2.2*a*) $\bar{\psi}$, P_1 satisfy

$$\bar{\psi}_{\bar{Y}}\bar{\psi}_{X\bar{Y}} - \bar{\psi}_X \bar{\psi}_{\bar{Y}\bar{Y}} = -P_1'(X). \tag{3.3b}$$

The boundary conditions on (3.3*b*) are

$$\left.\begin{aligned} \bar{\psi}_{\bar{Y}} &\sim \bar{Y} + A(X) \quad \text{as} \quad \bar{Y} \to \infty \\ \bar{\psi} &= 0 \quad \text{at} \quad \bar{Y} = f_e(X) \end{aligned}\right\} \tag{3.3c}$$

to match (3.3*a*) with (3.2*a*, *b*) and to satisfy (2.2*b*), in turn. Here $\bar{Y} = f_e(X)$ denotes the *effective* indentation shape, i.e., the unknown free streamline shape for $-\infty < X < X_1$, $f(X)$ for $X_1 < X < X_2$ and, finally, the unknown free streamline shape holding for $X > X_2$. Similarly, in zone III, where $y = 1 - l^{-2}\, \bar{\bar{Y}}$ with $\bar{\bar{Y}}$ of $O(1)$,

$$\psi = \psi(-\infty, 1) + l^{-4}\bar{\bar{\psi}}(X, \bar{\bar{Y}}), \quad P = l^{-4}P_2(X) \tag{3.4a}$$

to leading orders. Therefore $\bar{\bar{\psi}}$, P_2 are controlled by the inviscid boundary-layer equations, as in (3.3*b*), but

$$\left.\begin{aligned} \bar{\bar{\psi}}_{\bar{\bar{Y}}} &\sim \bar{\bar{Y}} - A(X) \quad \text{as} \quad \bar{\bar{Y}} \to \infty \\ \bar{\bar{\psi}} &= 0 \quad \text{at} \quad \bar{\bar{Y}} = -g_e(X). \end{aligned}\right\} \tag{3.4b}$$

In (3.4*b*) we have introduced (for future convenience) the possibility of a distortion of the upper wall also being present, of the form $y = 1 + l^{-2}g(X)$, and the subscript e stands again for 'effective', to account for the unknown free streamline shapes upstream and downstream (figure 2). Also, from (3.2*b*) we have the relation

$$P_2(X) = P_1(X) + qA''(X) \tag{3.5}$$

between the wall pressures and displacement.

The solution of $(3.3b, c)$ for layer II is $\bar{\psi} = \frac{1}{2}(\bar{Y}-f_e)(\bar{Y}+f_e+2A)$, giving

$$P_1 = -\tfrac{1}{2}(f_e+A)^2.$$

Similarly, the solution for layer III gives $P_2 = -\frac{1}{2}(g_e+A)^2$. Hence, with (3.5), we are left with the simple-looking, ordinary differential equation

$$2qA'' = (2A+f_e+g_e)(f_e-g_e) \tag{3.6}$$

for $A(X)$, $f_e(X)$, $g_e(X)$. In addition, however, (f_e+A) must be constant on the two free streamlines near the lower wall, from $(2.2b)$ and the solution above for P_1, while $(A+f)(A'+f') > 0$ during the attached part of the flow along $Y = f_e(X) = f(X)$, from $(2.2c)$, and the smooth separation condition of $(2.2e)$ is to be applied for a smooth indentation shape (3.1). Analogous constraints hold on (g_e+A).

Returning now to the case of an undistorted upper wall, $g = 0$, suggesting $g_e = 0$ and leaving $P_2 = -\frac{1}{2}A^2$ throughout, we split the solution of (3.6) for $-\infty < X < \infty$ into three parts, $X < X_1$, $X_1 < X < X_2$, $X > X_2$, where $X = X_1, X_2$ correspond to the positions $x = x_1, x_2$ of §2. First, for $X < X_1$, $P_1 = 0$ from $(2.2b)$ and (2.6), so that $f_e = -A$ and (3.6) becomes $2qA'' = -A^2$. This gives

$$A = \frac{-12q}{(X-d)^2} = -f_e, \quad P_2 = \frac{-72q^2}{(X-d)^4}, \quad P_1 = 0, \quad X < X_1, \tag{3.7a}$$

where d is a constant, to be found, such that $d > X_1$ to avoid an unrealistic singularity in $(3.7a)$. Note that $(3.7a)$ matches with (2.4) upstream and yields the result

$$D \approx ld \tag{3.7b}$$

for the variation of D in (2.3), while $P_2' < 0$ consistent with attached flow along $y = 1$. Second, for $X_1 < X < X_2$, $f_e(X) = f(X)$ is a given function and so (3.6) yields the linear differential equation

$$2qA'' = 2Af(X) + f^2(X) \tag{3.8}$$

for $A(X)$. Also $P_1 = -\frac{1}{2}(f+A)^2$ has to be monotonically decreasing with X, falling from zero at $X = X_1$ to an unknown value $-C_1 (C_1 > 0)$ at $X = X_2$. Third, for $X > X_2$, $P_1 = -C_1$ from (2.2), so that $f_e = -A \pm (2C_1)^{\frac{1}{2}}$ and (3.6) becomes

$$2qA'' = 2C_1 - A^2. \tag{3.9}$$

There are two solutions of (3.9) bounded at infinity, the one of interest to us being given by

$$\left.\begin{aligned} A &= -\left(\frac{C_1}{2}\right)^{\frac{1}{2}} \tilde{G}(\tilde{X}), \quad X = (2q^2/C_1)^{\frac{1}{4}}\tilde{X}, \\ \text{where} \qquad \tilde{G}(\tilde{X}) &= 2 - 6\,\mathrm{sech}^2((\tilde{X}+D_2)/2^{\frac{1}{2}}) \end{aligned}\right\} \tag{3.10}$$

and the constant D_2 is to be determined. The other solution has

$$\tilde{G} = 2 + 6\,\mathrm{cosech}^2((\tilde{X}+D_2)/2^{\frac{1}{2}})$$

but it is inadmissible since it implies $P_2'(X)\ (= -A(X)A'(X)) > 0$ in $X > X_2$ (it could apply if separation took place at the upper wall, however). Again, the choice

$$f_e(X) = -A(X) + (2C_1)^{\frac{1}{2}} \quad (X > X_2) \tag{3.11}$$

is necessary since, with (3.10), the other choice $f_e = -A - (2C_1)^{\frac{1}{2}}$ would yield $f_e < 0$, meaning that the free streamline would intersect the solid surface. Given the monotonic increase of $\tilde{G}$ with $\tilde{X}$ in (3.10), (3.11) shows that the distance of the free streamline from the wall increases monotonically in $X > X_2$ and so, from the smoothness requirement at the separation point $X = X_2$, it follows that the separation must occur ahead of the point of maximum constriction. Further, the ultimate distance of the free streamline from the wall as $X \to \infty$ is given by

$$f_e(\infty) = 2(2C_1)^{\frac{1}{2}} \tag{3.12}$$

from (3.10), (3.11).

Let us check now on the numbers of unknowns and conditions. The unknowns above are seven in number, comprising X_1, X_2, d, C_1, D_2 and the two arbitrary constants (β, γ, say) involved in the general solution of (3.8). The conditions imposed at $X = X_1$ are three: that A, A' and f_e be continuous, so that P_2, P_2' be continuous, and by definition, respectively. The governing equations (3.6), (3.8) then ensure continuity of P_2''. The remaining four conditions are those required at the separation point $X = X_2$ for a smooth indentation shape (cf. § 3.3 below): namely, that A and f_e' be continuous, that $P_1 = -C_1$ (by definition) and that $P_1' = 0$ (from (2.2*e*)). The first two conditions here ensure (also) that P_2, P_2', f_e and A' are all continuous at $X = X_2$, from the expressions above for P_1, P_2 and for f_e in terms of A. Hence the system is solvable in principle. Mathematically the seven constraints just above lead in turn to the following seven equations for X_1, X_2, d, C_1, $\tilde{G}_2$ ($\equiv \tilde{G}$ evaluated at $X = X_2$), β, γ:

$$\beta a_1(X_1+) + \gamma a_2(X_1+) + a_3(X_1+) = -12q(d-X_1)^{-2}, \tag{3.13a}$$

$$\beta a_1'(X_1+) + \gamma a_2'(X_1+) + a_3'(X_1+) = -24q(d-X_1)^{-3}, \tag{3.13b}$$

$$f(X_1+) = 12q(d-X_1)^{-2}; \tag{3.13c}$$

$$\beta a_1(X_2-) + \gamma a_2(X_2-) + a_3(X_2-) = -(C_1/2)^{\frac{1}{2}}\tilde{G}_2 \tag{3.14a}$$

$$f'(X_2-) = (C_1/2)^{\frac{3}{4}}(2-\tilde{G}_2)[(\tilde{G}_2+4)/3]^{\frac{1}{2}}q^{-\frac{1}{2}}, \tag{3.14b}$$

$$f(X_2-) + \beta a_1(X_2-) + \gamma a_2(X_2-) + a_3(X_2-) = (2C_1)^{\frac{1}{2}}, \tag{3.14c}$$

$$\beta a_1'(X_2-) + \gamma a_2'(X_2-) + a_3'(X_2-) = -f'(X_2-). \tag{3.14d}$$

In (3.13*a–c*), (3.14*a–d*) $a_1(X)$, $a_2(X)$ are complementary functions of (3.8) and $a_3(X)$ is a particular integral, while use of $\tilde{G}_2$ is preferred in place of D_2 and certain of the properties established between (3.7*a*) and (3.11) have been applied already.

For a given (smooth) indentation shape $f(X)$, then, the remaining task is to solve (3.8) for $a_1(X)$, $a_2(X)$, $a_3(X)$ and then determine X_1, X_2, d, C_1, $\tilde{G}_2$, β, γ from (3.13*a–c*), (3.14*a–d*). That task is tackled next, in § 3.2, for a range of specific shapes. The attached flow requirements that $P_1' < 0$ for $X_1 < X < X_2$ and $P_2' < 0$ for all X may be verified *a posteriori*. Also, we note that if the separation point $X = X_2$ is prescribed, e.g. at a slope discontinuity in $f(X)$, then only three conditions are to be imposed at $X = X_2$ and $f_e'(X)$ is discontinuous there in general (see § 3.3 below).

3.2. *Solutions for smooth indentations*

Solutions of (3.13*a–c*), (3.14*a–d*) were sought for the indentation shapes

$$f(X) = \frac{2}{1+k^2X^2} \quad (-\infty < X < \infty), \tag{3.15}$$

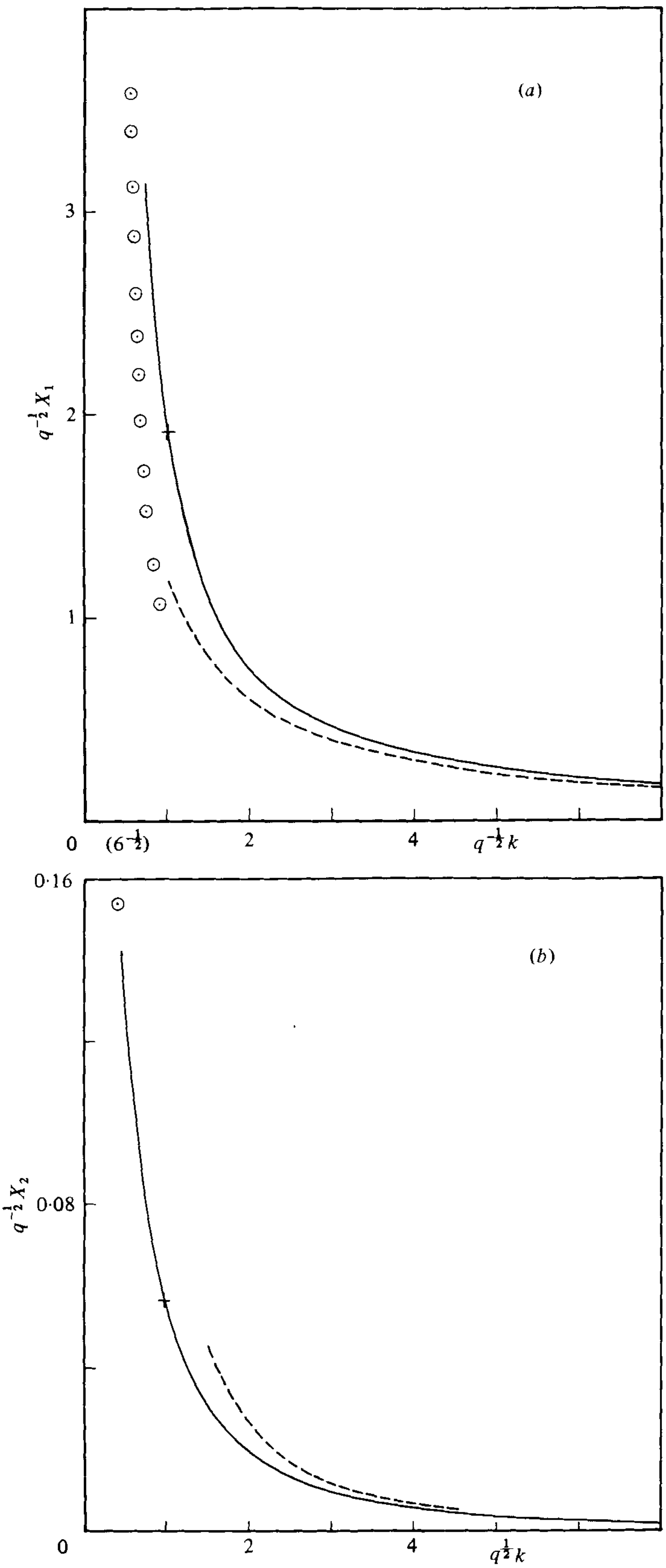

FIGURE 3. For legend see facing page.

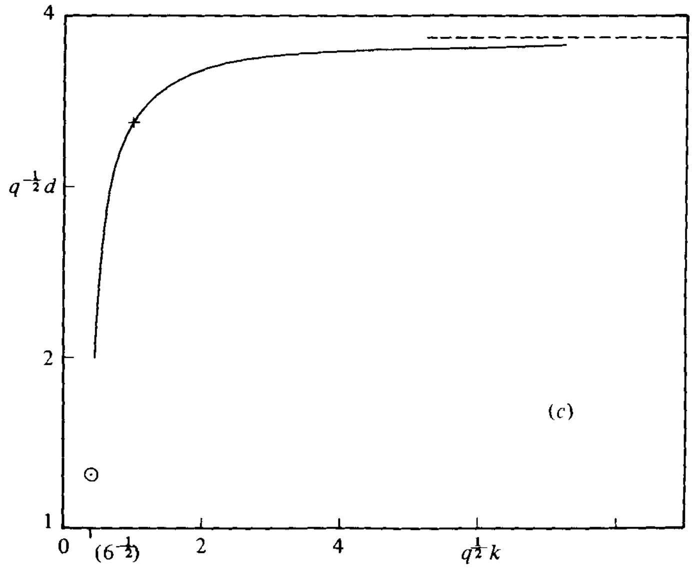

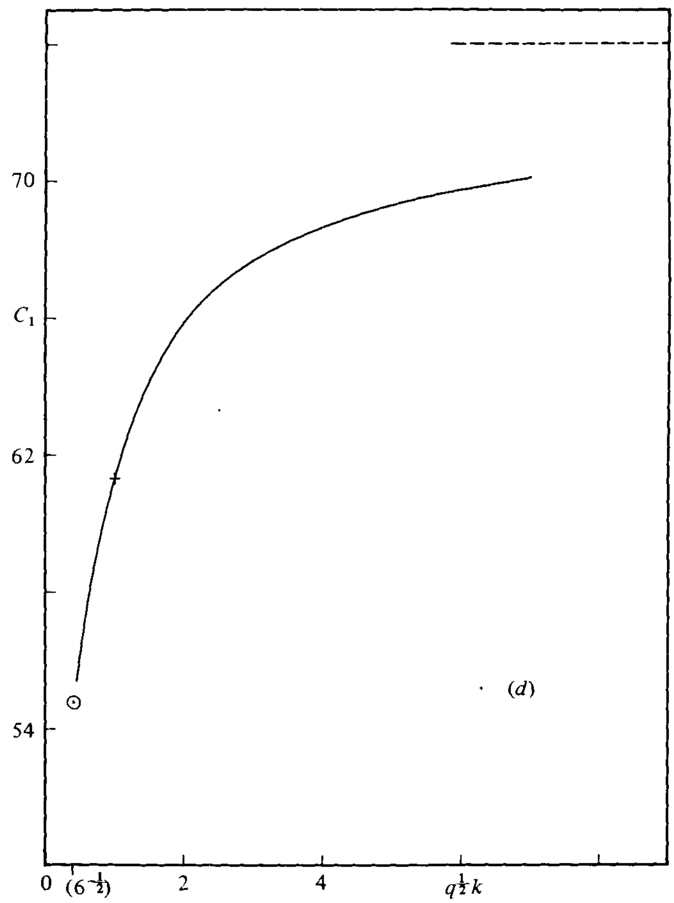

FIGURE 3. Solution graphs, versus $q^{\frac{1}{2}}k$, for (a) $q^{-\frac{1}{2}}X_1$, (b) $q^{-\frac{1}{2}}X_2$, (c) $q^{-\frac{1}{2}}$, (d) C_1 when the non-symmetric constriction is given by (3.15). In each case, – – –, +, ⊙⊙ give the analytic solutions for $k \to \infty$, $q^{\frac{1}{2}}k = 1$, $q^{\frac{1}{2}}k \to 6^{-\frac{1}{2}}+$ respectively [see (3.17), (3.19a, b), (3.20)–(3.21)].

$q^{\frac{1}{2}}k$	(∞)	7	6	5	4·25	4·00	3·75	3·50	3·25
$-q^{-\frac{1}{2}}X_1$	(0)	0·185	0·218	0·266	0·318	0·339	0·364	0·393	0·427
$-q^{-\frac{1}{2}}X_2$	(0)	0·0019	0·0026	0·0037	0·0050	0·0055	0·0062	0·0071	0·0081
$q^{-\frac{1}{2}}d$	(3·87)	3·828	3·819	3·807	3·798	3·788	3·781	3·774	3·764
C_1	(0·72)	0·701	0·697	0·693	0·691	0·686	0·685	0·682	0·679
$q^{\frac{1}{2}}k$	3·00	2·75	2·50	2·25	2·00	1·75	1·50	1·25	1·00
$-q^{\frac{1}{2}-}X_1$	0·468	0·517	0·578	0·655	0·755	0·889	1·083	1·385	1·920
$-q^{\frac{1}{2}-}X_2$	0·0094	0·0110	0·0130	0·0158	0·0193	0·0239	0·0306	0·0408	0·565
$q^{-\frac{1}{2}}d$	3·755	3·741	3·726	3·708	3·680	3·642	3·590	3·513	3·382
C_1	0·677	0·673	0·670	0·666	0·660	0·651	0·641	0·629	0·613
$q^{\frac{1}{2}}k$	0·90	0·80	0·70	0·60	0·55	0·50	0·45	$(6^{-\frac{1}{2}})$	
$-q^{-\frac{1}{2}}X_1$	2·271	2·782	3·600	5·149	6·629	9·50	18·25	(∞)	
$-q^{-\frac{1}{2}}X_2$	0·0654	0·0763	0·0900	0·107	0·118	0·129	0·142	(0·1540)	
$q^{-\frac{1}{2}}d$	3·302	3·194	3·041	2·805	2·631	2·390	2·015	(1·314)	
C_1	0·605	0·596	0·586	0·574	0·568	0·561	0·554	(0·5478)	

TABLE 1. The values of $q^{-\frac{1}{2}}X_1$, $q^{-\frac{1}{2}}X_2$, $q^{-\frac{1}{2}}d$, C_1 in the solution of (3·13*a–c*), (3.14*a–d*) with (3·8), (3·15), for various values of $q^{\frac{1}{2}}k$.

which indentations have height $2l^{-2}$ and length $O(k^{-1}l)$. The solutions depend only on the value of $q^{\frac{1}{2}}k$ and were obtained numerically for various values of $q^{\frac{1}{2}}k$. In fact, with (3.15) the differential equation (3.8) may be transformed into an associated Legendre equation, but solution of the latter equation is not relatively simple for general values of k and so instead we chose to solve (3.8) directly, using a Runge–Kutta scheme and various steplengths ΔX in X. The associated Legendre equation proves useful as a check on the numerical work at certain values of k, however, as shown below. In our numerical approach, a first guess was made for X_1, so that (3.13*c*) fixed d and (3.13*a*, *b*) then gave the values of $A(X_1+)$, $A'(X_1+)$. Hence (3.8) could be integrated forward from $X = X_1+$ to the station $X = X_2$ determined by (3.14*d*), with the values of C_1, $\tilde{G}_2$ then following from (3.14*c*), (3.14*a*) respectively, and the satisfaction of (3.14*b*) could be tested. By iterating with the value of X_1, therefore, the complete solution of (3.13*a–c*), (3.14*a–d*) could be found to satisfactorily high accuracy. The solutions for the different values of k studied appeared to be unique and are summarized in figure 3(*a*)–(*d*) and in table 1.

The trends of the flow solutions as $q^{\frac{1}{2}}k$ varies are of interest and considerable importance. A decrease in $q^{\frac{1}{2}}k$ makes the indentation more gradual and as a result the upstream reattachment point ($X = X_1$) is pushed further upstream, and the separation point ($X = X_2$) is moved further ahead of the maximum constriction point ($X = 0$). Also, d decreases, so that (from (3.7*b*), (2.3)) the upstream separation point ($x = x_{\mathrm{sep}}$) is forced further upstream. Increasing $q^{\frac{1}{2}}k$ produces a more abrupt indentation, so that the upstream flow separation lasts for a shorter distance (X_1 and x_{sep} both increase, since d increases, but x_{sep} increases faster), while the separation point $X = X_2$ is forced towards the maximum constriction point. Indeed, the flow properties (implied by the numerical work) for $k \gg 1$ appear to be as follows. When $k \gg 1$,

$$\left.\begin{aligned} X_1 &= k^{-1}\bar{X}_1 + k^{-2}\bar{\bar{X}}_1 + \dots, \quad X_2 = k^{-1}\bar{X}_2 + k^{-2}\bar{\bar{X}}_2 + \dots, \\ A &= A_0(\bar{X}) + k^{-1}A_1(\bar{X}) + \dots; \end{aligned}\right\} \tag{3.16a}$$

C_1, $\tilde{G}_2$, d remain $O(1)$, and the critical length scale is $X = k^{-1}\bar{X}$. Then (3.8) with (3.15) yields $A_0 = \beta_0 \bar{X} + \gamma_0$, $A_1 = \beta_1 \bar{X} + \gamma_1$. It is soon apparent from (3.13*a–c*), (3.14*a–d*) that $\beta_0 = \bar{X}_2 = 0$, leaving (3.13*a–c*), (3.14*a–d*) in the form (to leading order in k^{-1})

$$\left.\begin{aligned} \gamma_0 = -12q/d^2, \quad \beta_1 = -24q/d^3, \quad 2/(1+\bar{X}_1^2) = 12q/d^2, \\ \gamma_0 = -(C_1/2)^{\frac{1}{2}}\tilde{G}_2, \quad -4\bar{\bar{X}}_2 = (C_1/2)^{\frac{3}{4}}(2-\tilde{G}_2)\left(\frac{\tilde{G}_2+4}{3}\right)^{\frac{1}{2}} q^{-\frac{1}{2}}, \\ (2C_1)^{\frac{1}{2}} = \gamma_0 + 2, \quad \beta_1 = 4\bar{\bar{X}}_2, \end{aligned}\right\} \tag{3.16b}$$

in turn. Manipulation of (3.16*b*) leads to the equation $(1-B)^3 = (2B-1)^2(1+B)$ for $B \equiv (C_1/2)^{\frac{1}{2}}$, the solution of which is $B = \frac{3}{5}$. Hence from (3.16*b*)

$$\left.\begin{aligned} C_1 \to (\tfrac{18}{25}), \quad d \to (15q)^{\frac{1}{2}}, \quad X_1 \approx -(\tfrac{3}{2})^{\frac{1}{2}}k^{-1}, \\ X_2 \approx -\frac{2}{75}\left(\frac{15}{q}\right)^{\frac{1}{2}} k^{-2}, \quad f_e(\infty) \to \tfrac{12}{5} \end{aligned}\right\} \tag{3.17}$$

are the asymptotic trends of the solution for $k \to \infty$. Comparisons between (3.17) and the numerical solutions for increasing k tend to be supportive of (3.17), as figure 3 shows. The behaviours in (3.17) are particularly important when shorter scale (i.e., moderately severe) indentations are considered in § 4 below.

The other extreme limit of the solutions occurs when $q^{\frac{1}{2}}k \to 6^{-\frac{1}{2}}+$, since for $q^{\frac{1}{2}}k < 6^{-\frac{1}{2}}$ the upstream decay of the indentation of (3.15) is slower than that of the free streamline shape in (3.7*a*), implying attached flow far upstream at least. In fact, when $q^{\frac{1}{2}}k < 6^{-\frac{1}{2}}$ the upstream separation is totally suppressed on the X scale and separation first occurs only at $X = X_2$. The crossover from separated to attached flow upstream takes place because the upstream reattachment point $X = X_1$ is forced asymptotically far upstream as $k \to (6q)^{-\frac{1}{2}}+$. Setting $q^{\frac{1}{2}}k = 6^{-\frac{1}{2}} + \epsilon$, with $0 < \epsilon \ll 1$, we have d, C_1, X_2, $\tilde{G}_2$ remaining $O(1)$ but X_1 is large and negative, in the form $X_1 = q^{\frac{1}{2}}(\epsilon^{-1}\bar{X}_1 + \bar{\bar{X}}_1 + \ldots)$. To leading order, therefore, the range of interest for (3.8) with (3.15) is $-\infty < X < X_2$. For X of $O(1)$, also $A = A_0 + \epsilon A_1 + \ldots$ and (3.8), (3.15) yield the governing equation

$$\frac{d^2A_0}{d\bar{X}^2} = \frac{12A_0}{(\bar{X}^2+6)} + \frac{72}{(\bar{X}^2+6)^2} \quad [\bar{X} \equiv q^{-\frac{1}{2}}X]. \tag{3.18a}$$

We define the complementary functions a_1, a_2 such that $a_1 \approx \bar{X}^{-3}$, $a_2 \approx \bar{X}^4$ for $X \to -\infty$, whereas $a_3 \approx -12\bar{X}^{-2}$. The satisfaction of (3.13*a–c*) is achievable only if $\gamma = 0$ (to leading order). Also, it can be shown that $|A_1| \ll X^{-2}$ as $X \to -\infty$. Hence (3.13*a–c*) are found to be self-consistent and yield, on expanding in powers of ϵ, the results

$$q^{\frac{1}{2}}\beta = -24d, \quad d = -6^{\frac{1}{2}}\bar{X}_1 \quad \text{for} \quad \epsilon \to 0+. \tag{3.18b}$$

Next, (3.14*a–d*) are unaltered when $\epsilon \to 0+$ except that to leading order we may set $\gamma = 0$, leaving four equations for β, C_1, $\tilde{G}_2$, X_2, given the solution of (3.18*a*). The solution of (3.18*a*) must satisfy

$$A_0 \approx -12\bar{X}^{-2} + \beta\bar{X}^{-3} + \ldots \quad \text{for} \quad \bar{X} \to -\infty, \tag{3.18c}$$

from above, and is given by $A_0 = \beta a_1 + a_3$, where

$$\left.\begin{aligned} -\tfrac{576}{35}a_1(\bar{X}) &= (6+\bar{X}^2)(6+5\bar{X}^2)(\theta+\tfrac{1}{2}\pi)/(24)^{\frac{1}{2}} + 13\bar{X} + \tfrac{5}{2}\bar{X}^3, \\ 8a_3(\bar{X}) &= -\tfrac{576}{35}a_1(\bar{X}).(5\bar{X} - 6^{\frac{1}{2}}.4\theta) - (6+\bar{X}^2)(5\bar{X}^2+6) \\ &\quad \times [5\bar{X}(\theta+\tfrac{1}{2}\pi)(24)^{-\frac{1}{2}} + \tfrac{5}{2} - (\theta+\tfrac{1}{2}\pi)^2 + (6+\bar{X}^2)^{-1}] \end{aligned}\right\} \tag{3.18d}$$

and $-\frac{1}{2}\pi < \theta = \tan^{-1}(6^{-\frac{1}{2}}\bar{X}) < \frac{1}{2}\pi$. These expressions for a_1, a_3 may now be substituted into the four constraints

$$\left.\begin{aligned} &\beta a_1(\bar{X}_2)+a_3(\bar{X}_2) = -\left(\frac{C_1}{2}\right)^{\frac{1}{2}}\tilde{G}_2, \quad \frac{-24\bar{X}_2}{(\bar{X}_2^2+6)^2} = \left(\frac{C_1}{2}\right)^{\frac{3}{2}}(2-\tilde{G}_2)\left(\frac{\tilde{G}_2+4}{3}\right)^{\frac{1}{2}}, \\ &\frac{12}{(\bar{X}_2^2+6)}-\left(\frac{C_1}{2}\right)^{\frac{1}{2}}\tilde{G}_2 = (2C_1)^{\frac{1}{2}}, \quad \beta a_1'(\bar{X}_2)+a_3'(\bar{X}_2) = \frac{24\bar{X}_2}{(\bar{X}_2^2+6)^2}, \end{aligned}\right\} \qquad (3.18e)$$

stemming from (3.14a–d), to leave algebraic equations determining β, C_1, $\tilde{G}_2$ and $\bar{X}_2\,(\equiv q^{-\frac{1}{2}}X_2)$. The solution of (3.18$e$) with (3.18$d$) was found numerically and gives

$$\beta = -31{\cdot}58, \quad C_1 = 0{\cdot}5478, \quad \tilde{G}_2 = 1{\cdot}805, \quad X_2 = -0{\cdot}1540q^{\frac{1}{2}}. \qquad (3.19a)$$

Hence from (3.18b) we have also

$$d \to 1{\cdot}314q^{\frac{1}{2}}, \quad X_1 \approx -0{\cdot}536q^{\frac{1}{2}}/(q^{\frac{1}{2}}k-6^{-\frac{1}{2}}) \qquad (3.19b)$$

when $q^{\frac{1}{2}}k \to 6^{-\frac{1}{2}}+$, which completes the analytical description of how the (first) reattachment point is pushed indefinitely far upstream on the present ($O(1)$) scale. Clearly, if ϵ were decreased to order $l\,Re^{-\frac{1}{7}}$ then that reattachment point would enter the $Re^{\frac{1}{7}}$ region of the upstream free interaction of Smith (1977a) leading to (2.3). Further slight decreases of ϵ, and the eventual disappearance of the upstream separation and reattachment, would then be governed mainly by the $Re^{\frac{1}{7}}$ region, although when ϵ becomes negative and much greater than $O(l\,Re^{-\frac{1}{7}})$ one would expect the attached flow to be controlled by (3.18d, e) again. Moreover, the effects of decreasing k (and hence ϵ) still further, by an $O(1)$ amount, can still be accounted for by the work of § 3.1 provided the existence of attached flow upstream is recognized then. Such details, however, and the way in which a match is achievable between the present structure and that of Smith (1976a, b) in the limit as $k \to 0$ (where the constriction becomes very slowly varying), need not be pursued in the present work. Comparisons (figure 3) between the asymptotes (3.19a, b) and the numerical solutions as $q^{\frac{1}{2}}k \to 6^{-\frac{1}{2}}+$ show a fair measure of agreement.

Finally in this sub-section a check on the numerical solutions may be provided for the value $q^{\frac{1}{2}}k = 1$. Then the solution of (3.8) with (3.15) is

$$A(X) = \beta\sec^2\theta+\gamma(\theta\sec^2\theta+\tan\theta)+\tfrac{1}{2}(\theta^2\sec^2\theta+2\theta\tan\theta+1)\,(X \equiv q^{\frac{1}{2}}\tan\theta) \qquad (3.20)$$

where $-\frac{1}{2}\pi < \theta_1 < \theta < \theta_2 < 0$, $X_1 = q^{\frac{1}{2}}\tan\theta_1, X_2 = q^{\frac{1}{2}}\tan\theta_2$. Substitution of (3.20) into the constraints (3.13a–c), (3.14a–d) and some manipulation leaves the three equations

$$\left.\begin{aligned} &-6^{\frac{1}{2}}\sin\theta_2E^3 = (2-E^2)(E^2+1)^{\frac{1}{2}}, \\ &-\theta_2+(2-E^{-2})\sin(2\theta_2) = -\theta_1+\sin 2\theta_1-(\tfrac{8}{3})^{\frac{1}{2}}\cos\theta_1[\equiv\gamma], \\ &2(E^{-2}-1)\cos^4\theta_2-\tfrac{1}{2}(\theta_2^2+\theta_2\sin 2\theta_2+\cos^2\theta_2)-(\theta_2+\tfrac{1}{2}\sin 2\theta_2)\gamma \\ &\qquad = -2\cos^4\theta_1-\tfrac{1}{2}(\theta_1^2+\theta_1\sin 2\theta_1+\cos^2\theta_1)-(\theta_1+\tfrac{1}{2}\sin 2\theta_1)\gamma, \end{aligned}\right\} \qquad (3.21)$$

for $E(\equiv(2/C_1)^{\frac{1}{4}}\cos\theta_2), \theta_2, \theta_1$. The solution of (3.21) gives

$$\tan\theta_1 = -0{\cdot}0565, \quad \tan\theta_2 = -1{\cdot}92, \quad C_1 = 0{\cdot}613$$

to the number of significant figures shown. This agrees favourably with the numerical solution shown in table 1 for $q^{\frac{1}{2}}k = 1$.

3.3. *Solutions for non-smooth indentations*

The particular non-smooth indentation shapes to be studied here are given by

$$f(X) = \begin{cases} X(0 < X < X_3), \quad X_3(X_3 < X < X_4), \quad X_3+X_4-X(X_4 < X < X_3+X_4); \\ 0 \quad \text{otherwise}. \end{cases} \tag{3.22}$$

As well as illustrating the application of the slowly varying theory to non-smooth indentations, the ramp-step (3.22) also bears strong resemblance to an experimental set-up for a non-symmetrically constricted channel flow currently under investigation at Cambridge University (T. J. Pedley, private communication 1979). With (3.22), the solution of (3.8) is

$$\hat{A} = \beta\, Ai\,(\hat{X}) + \gamma\, Bi\,(\hat{X}) - \tfrac{1}{2}\hat{X} \tag{3.23}$$

where Ai, Bi are the solutions of Airy's equation, $A = q^{\frac{1}{3}}\hat{A}$ and $X = q^{\frac{1}{3}}\hat{X}$. The conditions at $X = X_1(0 < X_1 < X_3)$ are as in (3.13*a*–*c*), but at the separation point, which we assume immediately to be at the convex corner $X = X_2 = X_3$, only the three conditions, that A, A' be continuous and $P_1 = -C_1$ (by definition), are relevant. These three are required for continuity of f_e, P_2, P_2', and P_1; f_e' is discontinuous in general (due to the corner, prescribing the position $X = X_2$). Applying the six conditions and manipulating we obtain two equations, with $W \equiv (Ai\,Bi' - Ai'\,Bi)(\hat{X})$,

$$\begin{aligned} &3^{-\frac{1}{2}}\hat{X}_1^{\frac{3}{2}}\, Bi(\hat{X}_1) - \tfrac{1}{2}\hat{X}_1\, Bi'(\hat{X}_1) - \tfrac{1}{2}\, Bi(\hat{X}_1) \\ &\qquad = -\tfrac{1}{2}\hat{X}_2\, Bi'(\hat{X}_2) - \tfrac{1}{2}\, Bi(\hat{X}_2) + 2\tilde{E}\, Bi'(\hat{X}_2) + Bi(\hat{X}_2)\,(4\tilde{E} - \hat{X}_2)\,\tfrac{1}{3}(2\tilde{E} + \hat{X}_2)]^{\frac{1}{2}}, \end{aligned} \tag{3.24a}$$

$$\begin{aligned} &Bi(\hat{X}_2)\,[-Ai(\hat{X}_1)\,(3^{-\frac{1}{2}}X_1^{\frac{3}{2}} - \tfrac{1}{2}) + \tfrac{1}{2}\hat{X}_1\, Ai'(\hat{X}_1)] \\ &\qquad = (2\tilde{E} - \tfrac{1}{2}\hat{X}_2)\, W - Ai(\hat{X}_2)\,[3^{-\frac{1}{2}}\hat{X}_1^{\frac{3}{2}} - \tfrac{1}{2}\hat{X}_1\, Bi'(\hat{X}_1)/Bi(\hat{X}_1) - \tfrac{1}{2}]\, Bi(\hat{X}_1), \end{aligned} \tag{3.24b}$$

for $\hat{X}_1(= q^{-\frac{1}{3}}X_1)$ and $\tilde{E}(= q^{-\frac{1}{3}}(\frac{1}{2}C_1)^{\frac{1}{2}})$ for a given value of $\hat{X}_2(= q^{-\frac{1}{3}}X_3)$. The numerical solution of (3.24*a*, *b*) for $\hat{X}_1$, $q^{-\frac{2}{3}}C_1$ (and hence $q^{-\frac{1}{3}}d$, $\tilde{G}_2$ from (3.13*a*–*c*) and above) is presented in figure 4 for various values of $q^{-\frac{1}{3}}X_3$. The increase of X_1 and the decrease of d with increasing X_3 (i.e. increasing height of step) seem sensible physically as they represent an enhancement of the upstream influence. We would emphasize here too the typical property of free streamline theory, that the indentation shape beyond $X = X_3$ exerts no influence at all on the flow features to leading order provided the shape there does not protrude through the downstream free streamline.

For a relatively small ramp-step, where $X_3 \ll 1$, (3.24*a*, *b*) may be solved analytically. Then X_1 and E both become $O(X_3)$ and after working through (3.24*a*, *b*) to orders $X_3^{\frac{5}{2}}$ we find that

$$X_1 \approx \tfrac{2}{5}X_3, \quad \tilde{E} \approx \tfrac{3}{10}X_3, \quad C_1 \approx \tfrac{9}{50}X_3^2, \quad \tilde{G}_2 \to \tfrac{4}{3}, \quad d \approx (30q/X_3)^{\frac{1}{2}} \quad \text{for} \quad X_3 \to 0. \tag{3.25}$$

Thus when X_3 is small the upstream free streamline intersects the ramp step at $\frac{2}{5}X_3$, while the downstream free streamline emanates from the corner at $X = X_3$ with a very small slope, of $\frac{8}{9}(\frac{3}{10}X_3)^{\frac{3}{2}}$, from (3.25), on the $X - \overline{Y}$ scalings, and ultimately tends to a distance of $\frac{6}{5}X_3$ from the undisturbed wall, from (3.25) with (3.12). Comparisons between (3.25) and the calculations are presented in figure 4. For a relatively large ramp-step, $X_3 \gg 1$, the solution is again obtainable analytically. We find that X_1, d, β remain $O(1)$, $\gamma \to 0$ and $\hat{X}_1$ satisfies

$$(\tfrac{4}{3})^{\frac{1}{2}}\hat{X}_1^{\frac{3}{2}} - \hat{X}_1\, Ai'(\hat{X}_1)/Ai(\hat{X}_1) = 1, \tag{3.26}$$

which gives $X_1 = 0{\cdot}5432q^{\frac{1}{3}}$. Hence $d \to 5.236q^{\frac{1}{3}}$ for $X_3 \to \infty$, and $\tilde{E} \approx \frac{1}{4}\hat{X}_3$.

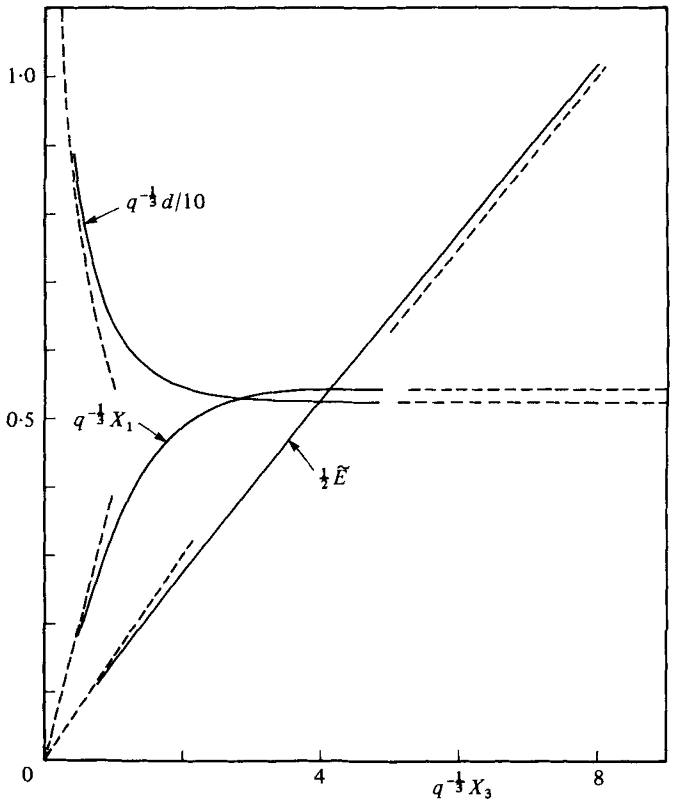

FIGURE 4. The dependence of X_1, d, $\tilde{E}$ on X_3 in the ramp-step case. The dashes indicate the asymptotes stemming from (3.25), (3.26).

In §4 below we discuss the implications of the long scale theory and solutions of §§3.1–3.3 for slender, and for moderately severe, distortions of the channel. The implications for curved or cornered channel flows are then followed through in §§5, 6.

4. Implications for slender or moderately severe constrictions

For slender, and for moderately severe, non-symmetric constrictions of the channel flow the solutions of the nonlinear problem posed in §2 have strong connections with the slowly varying theory of §3. We consider first (in §4.1) the slender case, since that is easier to deal with, and then consider the moderately severe case in §4.2. Also, we take the upper wall to be undistorted again, to avoid undue complications, and further suppose the lower wall distortion to be reasonably smooth.

4.1. *Slender constrictions*

'Slender' here refers to a non-symmetric constriction whose typical streamwise length L is large ($1 \ll L \ll Re^N$ as in §3) but whose typical height is of $O(1)$. Hence the lower wall is described by $y = \hat{F}(\hat{X})$, say, where $x = L\hat{X}$ and $\hat{F}$ is of $O(1)$ or less ($0 \leqslant \hat{F} < 1$), whereas the upper wall remains straight (at $y = 1$). For convenience we suppose that the constriction is wedge-like at its beginning (at $\hat{X} = 0$, say), so that

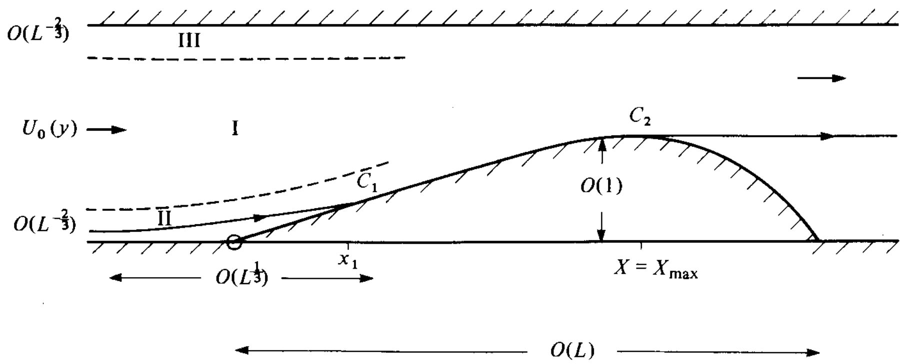

FIGURE 5. The overall structure of the motion through a slender constriction.

$\hat{F}(\hat{X}) \approx \hat{\alpha}\hat{X}$ for $\hat{X} \to 0+$, $\hat{F}(\hat{X}) = 0$ for $\hat{X} < 0$, with $\hat{\alpha}$ of $O(1)$. Other forms for the beginning of the constriction are readily analysable, as are constrictions incorporating some distortion of the upper wall, in principle.

Near $\hat{X} = 0$, therefore, the constriction takes the wedge shape $y = \hat{\alpha}x/L(x > 0)$, $0(x < 0)$. The theory of § 3.1 above then suggests that the lengthscale $x = O(L^{\frac{1}{3}})$ must be considered, to explain the way in which the fluid flow anticipates (in $x < 0$) the presence of the constriction in $x > 0$. On that $O(L^{\frac{1}{3}})$ scale, identifying $\hat{\alpha}^{-\frac{1}{3}}L^{\frac{1}{3}}$ with l we see that the three-tiered structure of § 3.1 is set up (figure 5), leaving the governing equation (3.8) (with $f(X) = X$ now) for the attached part of the flow, $X > X_1$: we expect separation upstream, in the form (3.7a), of course, but beyond the reattachment at $X = X_1$ the flow is expected to remain attached throughout the $X = O(1)$ scale. With $f = X$, and requiring boundedness as $X \to \infty$, we obtain the solution

$$A(X) = \beta\, Ai(Xq^{-\frac{1}{3}}) - \tfrac{1}{2}X \tag{4.1}$$

of (3.8) for $X > X_1$. The three conditions at $X = X_1$ are given by (3.13a–c), with $\gamma = 0$, $a_1(X) \equiv Ai(Xq^{-\frac{1}{3}})$, $a_3(X) \equiv -\tfrac{1}{2}X$, and they yield the values of X_1, d, β. In particular, $X_1q^{-\frac{1}{3}}$ satisfies (3.26) as might be expected, so that from just below (3.26) the results

$$x_1 \approx 0{\cdot}5432(Lq/\hat{\alpha})^{\frac{1}{3}}, \quad D \approx 5{\cdot}236(Lq/\hat{\alpha})^{\frac{1}{3}}, \tag{4.2}$$

determine the upstream reattachment and separation positions (by use of (2.3)). Far downstream on this scale, as $X \to \infty$, $A \sim -\tfrac{1}{2}X$ from (4.1) and a match is achieved then with the simpler theory of Smith (1976a) in the sense that the core displacement $(-A)$ becomes equal to the average displacement of the walls.

Further downstream (figure 5), on the $O(L)$ scale in x, the solution of (2.2a–e) becomes single-structured and is simplified by the fact that, in effect, $\partial/\partial x \ll \partial/\partial y$. Hence to leading order U, V, P satisfy the inviscid boundary-layer equations, with $P = P(X)$ now independent of y (cf. § 3), which give on integration the equation (cf. Pretsch 1944; Cole & Aroesty 1968)

$$1 - \hat{F}_e(\hat{X}) = \int_0^{\psi_0(1)} \frac{d\psi_0}{[U_0^2(\psi_0) - 2P(\hat{X})]^{\frac{1}{2}}} \tag{4.3}$$

for the determination of $P(\hat{X})$, given $\hat{F}_e(\hat{X}) = \hat{F}(\hat{X})$ for attached flow or, on free streamlines, for $\hat{F}_e(\hat{X})$ given $P(\hat{X}) = \text{constant}$. The match with (4.1) near $\hat{X} = 0+$ may be verified readily from (4.3). Further, since $P(\hat{X})$ is constant beyond the separation point $x = x_2$, or $\hat{X} = \hat{X}_2$, the integral (4.3) shows that $\hat{F}_e(\hat{X})$ must also be constant there. Then smoothness requirements at the separation point imply the results

$$\hat{X}_2 = \hat{X}_{\max}, \quad \hat{F}_e(\hat{X}) = \hat{F}(\hat{X}_{\max}) \quad \text{for} \quad \hat{X} > \hat{X}_{\max} \tag{4.4}$$

separation occurring at the point $\hat{X} = \hat{X}_{\max}(x = x_{\max})$ of maximum constriction (as in Smith 1979*a*). We note in passing that an alternative form of the solution involves solving $\psi_{yy} = \zeta(\psi)$ for ψ and leads to the same conclusion (4.4).

4.2. *Moderately severe constrictions*

'Moderately severe' here describes a constriction of $O(1)$ typical streamwise length but whose typical height h is small (strictly $1 \gg h \gg Re^{-N}$, as in § 3). For symmetrically constricted flows the moderately severe case can be treated by a linearization, about the oncoming flow (2.6), involving perturbations of order h^2 in the core (Smith 1979*a*, § 3). For our non-symmetrically constricted channel flow, however, before an analogous treatment is attempted some prior thoughts are necessary in view of the limiting properties of the solutions of § 3.2 when $k \to \infty$ there. One would expect those limiting properties, which correspond to a shortening of the indentation's characteristic length scale from $O(l)$ to $O(lk^{-1})$ but with the maximum height remaining $2l^{-2}$, to give us a guide to the flow properties for a moderately severe non-symmetric constriction and so it proves. Thus, formally identifying the height h with l^{-2} and letting $k \to O(l)$, so that the slowly varying severe indentation of § 3.2 tends towards a moderately severe kind, we conclude from (3.16*a*)–(3.17) that even during a moderately severe constriction the three-tiered structure of §§ 3.1–3.2 is still set up on the long scale $x = O(h^{-\frac{1}{2}})$, upstream and downstream of the indentation, while (in contrast and as might be expected *ab initio*) the details of reattachment and separation from the indentation occur on the shorter length scale ($O(1)$) of the indentation itself. Moreover, the perturbations of the core flow are now $O(h) + O(h^{\frac{3}{2}})$ [from (3.2*a*) with $l \to O(h^{-\frac{1}{2}})$ and from (3.16*a*) with $k \to O(h^{-\frac{1}{2}})$], much larger than the perturbations occurring in symmetrically constricted flows (Smith 1979*a*), and the displacement D in (2.3)–(2.5) becomes $O(h^{-\frac{1}{2}})$ from (3.7*b*) with $l \to O(h^{-\frac{1}{2}})$.

The flow structure resulting for moderately severe constriction is shown schematically in figure 6. In regions I–III, however, the solutions are essentially those of §§ 3.1–3.2 upstream of reattachment and so, effectively, are merely the continuation of (2.4). Thus, with $x = h^{-\frac{1}{2}}\bar{x}$ and $\bar{x}$ of $O(1)$ and negative,

$$F_1 = 12q/(h^{-\frac{1}{2}}(\bar{x}-\bar{d}))^2, \tag{4.5a}$$

$$P(\bar{x}, y) = -72q(h^{-\frac{1}{2}}(\bar{x}-d))^{-4}\int_0^y U_0^2(\bar{y})\,d\bar{y}, \tag{4.5b}$$

$$D = h^{-\frac{1}{2}}\bar{d}, \tag{4.5c}$$

to leading order. Hence the match upstream with (2.4) is achieved.

Then, closer to the indentation, where regions IV–VI are set up with x of $O(1)$, the solution of (2.2*a*) in region IV ($0 < y < 1$) takes the form

$$\psi = \psi_0(y) + h\tilde{\psi}_1(x, y) + h^{\frac{3}{2}}\tilde{\psi}_2(x, y) + O(h^2), \tag{4.6a}$$

$$P = h^2\tilde{P}_1(x, y) + h^{\frac{5}{2}}\tilde{P}_2(x, y) + O(h^3). \tag{4.6b}$$

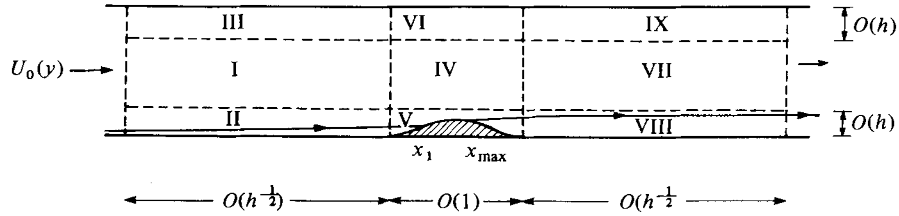

FIGURE 6. Schematic diagram of the flow structure produced by a moderately severe constriction.

Here, from (2.2a), or the vorticity equation just below (2.2a), $\tilde{\psi}_1$, $\tilde{\psi}_2$ satisfy the linear equations of motion

$$\nabla^2\tilde{\psi}_1 = \tilde{\psi}_1\zeta'(\psi_0), \quad \nabla^2\tilde{\psi}_2 = \tilde{\psi}_2\zeta'(\psi_0) \tag{4.7a}$$

and, from (2.2b–d) and Taylor series expansion,

$$\tilde{\psi}_1 = \tilde{\psi}_2 = 0 \quad \text{on} \quad y = 0, 1. \tag{4.7b}$$

Further, the match with (4.5a, b) requires

$$\tilde{\psi}_1 \to -\tilde{A}_1\psi_0'(y), \quad \tilde{\psi}_2 \sim -\tilde{A}_2 x\psi_0'(y) \quad \text{as} \quad x \to -\infty, \tag{4.7c}$$

where

$$\tilde{A}_1 = 12q/d^2; \quad \tilde{A}_2 = 24q/d^3. \tag{4.7d, e}$$

We notice that the match with (2.5a–c) upstream is achieved not by (4.7c–e) but by the longer scale adjustment described by (4.5a–c) further upstream. Downstream, as $x \to \infty$, no exponential growth is to be allowed. The unique solutions of (4.7a–c) are simply

$$\tilde{\psi}_1 = -\tilde{A}_1\psi_0'(y), \quad \tilde{\psi}_2 = -(\tilde{A}_2 x + \tilde{B}_2)\psi_0'(y), \tag{4.8}$$

where the constant $\tilde{B}_2$ is unknown. Strictly, the solutions in the wall regions V, VI should perhaps be expanded separately from the core expansion (of (4.6a)) next, as was done in § 3.1, but the solutions in V, VI are really the continuations of (4.6a, b), re-written in terms of local co-ordinates $Y_1 = h^{-1}y$ and $Y_2 = (1-y)h^{-1}$ respectively. Therefore V, VI yield the results (similarly to § 3.1)

$$\tilde{P}_1(x, 0) = -\tfrac{1}{2}(f_e(x) - \tilde{A}_1)^2, \quad \tilde{P}_1(x, 1) = -\tfrac{1}{2}\tilde{A}_1^2, \tag{4.9}$$

where $y = hf_e(x)$ is the effective indentation shape (comprising the upstream free streamline, the actual indentation and the downstream free streamline in order, as in § 3.1), so that $F_1(x) \approx hf_e(x)$ for $x < x_1$, and the actual indentation is given by

$$y = h\tilde{f}(x). \tag{4.10}$$

From the constant pressure requirement (2.2b) in $x < x_1$, (4.9) yields the result

$$f_e(x) = \tilde{A}_1 \quad \text{for all} \quad x < x_1, \tag{4.11}$$

which matches upstream with (4.5a) (as $\bar{x} \to 0-$). Continuity of $f_e(x)$ at $x = x_1$ then imposes

$$\tilde{A}_1 = f(x_1). \tag{4.12}$$

Similarly, the constant pressure requirement (2.2b) in $x > x_2$ shows that $f_e(x)$ is constant beyond separation, from (4.9), which with the smooth separation condition (2.2e) implies that to leading order

$$x_2 = x_{\max}, \quad f_e(x) = f_{\max} \quad \text{for} \quad x > x_{\max}. \tag{4.13}$$

The separation at maximum constriction ($f(x_{\max}) = f_{\max}$), followed by the straight separation line, in (4.13), are reminiscent of the symmetric flow properties of Smith (1979*a*). Also, the constant pressure $\tilde{P}_1(x, 0) = -C_1$ beyond separation is related to the unknown constant $\tilde{A}_1$ by the equation

$$(f_{\max} - \tilde{A}_1) = (2C_1)^{\frac{1}{2}}, \tag{4.14}$$

from (4.9). However, we do not have enough conditions yet to fix the unknown values of C_1, $\tilde{A}_1$, $\bar{d}$ and x_1. Only three relations, (4.7*d*), (4.12), (4.14), can be established between the above four unknowns on this $O(1)$ length scale.

Remarkably enough, to determine the remaining unknowns, including even the reattachment position $x = x_1$, the longer scale flow (see figure 5) beyond the constriction, where $x = h^{-\frac{1}{2}}\bar{x}$ but with $\bar{x}$ positive and $O(1)$, must be accounted for again. There a three-tiered structure (VII–IX) analogous to that of § 3.1 is promoted. Indeed, replacing l in § 3.1 by $h^{-\frac{1}{2}}$ and X by $\bar{x}$, we may go straight through from (3.2*a*) to the equation (3.6) for the negative displacement A and thence to (3.9) (and its solution (3.10)) and (3.11), since now in $\bar{x} > 0$ the flow is separated in the form (3.11). Matching the core solutions for ψ and their x derivatives [the governing equations (2.2*a*) then guarantee matching of lower order x derivatives of ψ], from the $O(1)$ scale (given by (4.8)) to the $O(h^{-\frac{1}{2}})$ scale downstream (given by (3.2*a*, *b*), as just described), then requires $A(\bar{x}) \to -\tilde{A}_1$, $dA/d\bar{x} \to \tilde{A}_2$ as $\bar{x} \to 0+$, or from (3.10)

$$\tilde{A}_1 = (\tfrac{1}{2}C_1)^{\frac{1}{2}}\,\tilde{G}_2, \tag{4.15a}$$

$$\tilde{A}_2 = (\tfrac{1}{2}C_1)^{\frac{3}{4}}\,(2-\tilde{G}_2)\,[\tfrac{1}{3}(\tilde{G}+4)]^{\frac{1}{2}}\,q^{-\frac{1}{2}}. \tag{4.15b}$$

Now (4.15*a*, *b*) together with (4.7*d*, *e*) (4.12), (4.14) provide the necessary six equations to fix C_1, $\tilde{A}_1$, $\bar{d}$, x_1, $\tilde{A}_2$ and $\tilde{G}_2$. Since x_1 appears only in equation (4.12) the other five equations yield C_1, $\tilde{A}_1$, $\bar{d}$, $\tilde{A}_2$, $\tilde{G}_2$ independently of x_1 and we find the unique solution

$$C_1 = \tfrac{9}{50}f^2_{\max}, \quad \tilde{A}_1 = \tfrac{2}{5}f_{\max}, \quad \bar{d} = \left(\frac{30q}{f_{\max}}\right)^{\frac{1}{2}}, \quad \tilde{A}_2 = (\tfrac{3}{5}f_{\max})^{\frac{3}{2}}/(3q)^{\frac{1}{2}}, \quad \tilde{G}_2 = \tfrac{4}{3}. \tag{4.16}$$

Then (4.12) determines x_1 from the relation $f(x_1) = \frac{2}{5}f_{\max}$. Clearly (4.16) is the direct extension of the results in (3.17) (for $k \gg 1$), generalized to arbitrary smooth shapes of indentation [so that, in particular, a refinement of the prediction (4.13) for the separation position $x = x_2$ could be made as in (3.17)]. The simple, universal, form of the results in (4.16) for smooth moderately severe indentations seems nonetheless intriguing. According to (4.16) and (4.13), for any value of q the upstream free streamline attaches to the indentation at the station where the indentation height reaches 40 % of its maximum value, the flow then separates at the maximum constriction point, and ultimately the downstream free streamline lies at a normal distance from the wall of 120 % of the maximum constriction height. Other features, such as wall pressure values (see (4.9), (4.14), (4.16)) and the upstream separation position (see (2.3), (4.5*c*), (4.16)), are equally striking, as are the relative complexity of the present structure (figure 6) and the relative simplicity of the core-flow results ((4.7)–(4.8)) compared with the symmetrical-flow case (Smith 1979*a*).

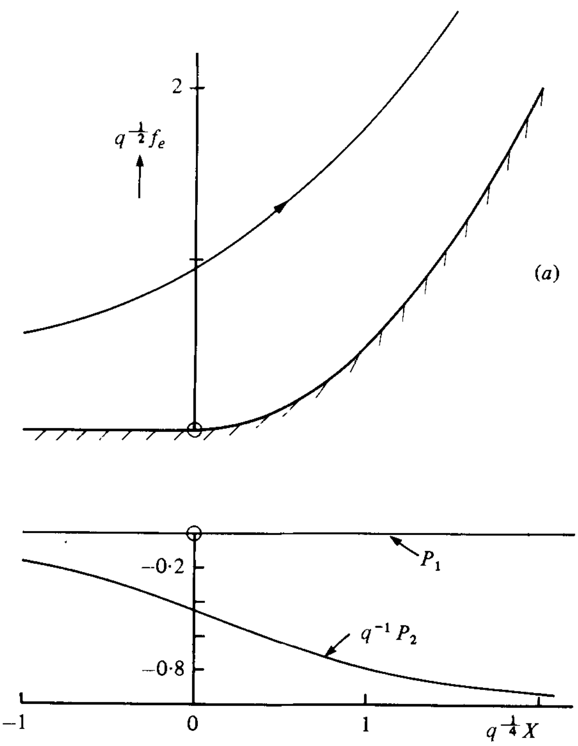

FIGURE 7. (*a*) The free streamline shape f_e (→) compared with the wall shape (⫽⫽), and (*b*) the upper and lower wall pressures P_2, P_1, versus X for the curved channel.

5. The curved channel

This section and the next are concerned with two fundamental flow problems which involve unbounded non-symmetric distortions of the original channel walls but which, nevertheless, are closely related to the theory of §§ 2 and 3.1 above.

To be considered first is the flow response due to an abrupt (and severe) curving of the channel at $x = 0$, with the lower and upper walls prescribed by $y = 0$ $(x < 0)$, $\kappa x^2/2 (x > 0)$ and $y = 1 (x < 0)$, $1 + \frac{1}{2}\kappa x^2 (x > 0)$, respectively; some interesting qualitative comments on this problem were made by Goldstein (1938, pp. 85–87), while the analogous problems for very mild curvatures were analysed by Bates (1978) in abruptly curving channel flow and by Smith (1976*c*) in abruptly curving pipe flow. The constant $\kappa (> 0)$ above is of order unity as far as the Reynolds-number expansion of (2.1) is concerned, so that the general approach in § 2 can be adopted subject to the inclusion of the upper-wall distortion. Following some trial and error we conclude that, for a moderately severe curving, where $0 < \kappa \ll 1$, the flow separates far upstream at the lower wall (by means of the free interaction leading to (2.3)–(2.5*c*)) and remains separated there throughout the length scale of present interest (i.e. $-Re^{\frac{1}{7}} \ll x \ll Re$), whereas the flow at the upper wall remains attached throughout (figure 7). A similar conclusion is expected to hold for an extensive range of severe curvatures ($\kappa = O(1)$).

For $0 < \kappa \ll 1$ the flow solution assumes the long scale structure of § 3.1 but with l being replaced by $\kappa^{-\frac{1}{2}}$ and $f(X)$, $g(X)$ both being given by zero for $X < 0$, $\frac{1}{2}X^2$ for $X > 0$ (here $X = \kappa^{\frac{1}{2}}x$). Hence $A(X)$ satisfies (3.6) again, and, for $X < 0$, (3.7*a*) gives the solution. For $X > 0$ we still have $f_e = -A$, $P_1 = 0$ but now $g_e = g = \frac{1}{2}X^2$, so that A satisfies the equation

$$2qA'' = -(A + \tfrac{1}{2}X^2)^2 \tag{5.1}$$

from (3.6). The solution of (5.1) (bounded as $X \to \infty$) follows by setting $A + \frac{1}{2}X^2 = B$, leaving B governed by (3.9) and its solution (3.10) provided B, q are written now instead of A, C_1. Since no points of separation or reattachment occur on the $X = O(1)$ scale the only (two) conditions necessary are the continuity of A, A' at $X = 0$; the governing equations then guarantee continuity of A'', A''' there. The two conditions impose the two relations

$$-(q/2)^{\frac{1}{2}}\,\tilde{G}_0 = -12q/d^2, \tag{5.2a}$$

$$-q^{\frac{1}{2}}2^{-\frac{3}{2}}(2-\tilde{G}_0)\,[\tfrac{1}{3}(\tilde{G}_0+4)]^{\frac{1}{2}} = -24q/d^3, \tag{5.2b}$$

controlling the values of $\tilde{G}_0(\equiv \tilde{G}$ at $X = 0)$ and d, from (3.7a), (5.1) and (3.9), (3.10). The solution of (5.2a, b) is unique and is

$$d = 3(2q)^{\frac{1}{4}}, \quad \tilde{G}_0 = \tfrac{4}{3}. \tag{5.3}$$

The value of d here fixes the upstream separation position, through (3.7b) and (2.3), while the $\tilde{G}_0$ value implies that at $X = 0$ the free streamline lies at a distance (on the $\bar{Y}$ scale) of $\frac{2}{3}(2q)^{\frac{1}{2}}$ from the lower wall. Also, as $X \to \infty$ we have

$$f_e(X) = -A(X) \approx \tfrac{1}{2}X^2 + (2q)^{\frac{1}{2}}, \tag{5.4}$$

so that the free streamline eventually becomes parallel to both walls and its normal distance from the lower wall tends to the value $(2q)^{\frac{1}{2}}$ on the $\bar{Y}$ scale, i.e. $(2q\kappa)^{\frac{1}{2}}$ in terms of y. Figure 7 presents the solutions for the free streamline shape and the wall pressures, which have the asymptotic forms

$$P_2 \to -q, \quad P_1 = 0 \quad \text{as} \quad X \to \infty. \tag{5.5}$$

The persistence of this pressure difference across the downstream channel is required to maintain the curved flow there.

6. The cornered channel

The final form of severe distortion that we consider concerns a channel suffering an abrupt cornering, such that its lower wall is described by $y = 0$ $(x < 0)$, $y = \alpha x$ $(x > 0)$ and its upper wall by $y = 1$ $(x < 0)$, $y = 1 + \alpha x$ $(x > 0)$. Here $\alpha(> 0)$ is of $O(1)$ with respect to the Reynolds number and so the general theory of § 2 applies but modified owing to the presence of the upper wall distortion and to the corner there (which, as it turns out, prescribes a separation point). As in the previous section the upstream separation described in § 2 by (2.3) and (2.4)–(2.5c) is expected to occur along the lower wall, of course. However, thereafter several questions immediately arise for the subsequent flow development because of the possibility of flow separation at the upper wall combined with the possibilities of flow reattachments at finite distances downstream on both walls (cf. § 5). After some trial and error we find that (in the moderately severe case $\alpha \ll 1$, at least, but probably in the general severe case ($\alpha = O(1)$) also) self-consistency is provided only by the following account which postulates separation occurring at the upper corner $x = 0$, an ensuing reattachment at the lower wall, but no reattachment (on a finite scale in x) at the upper wall: see figure 8.

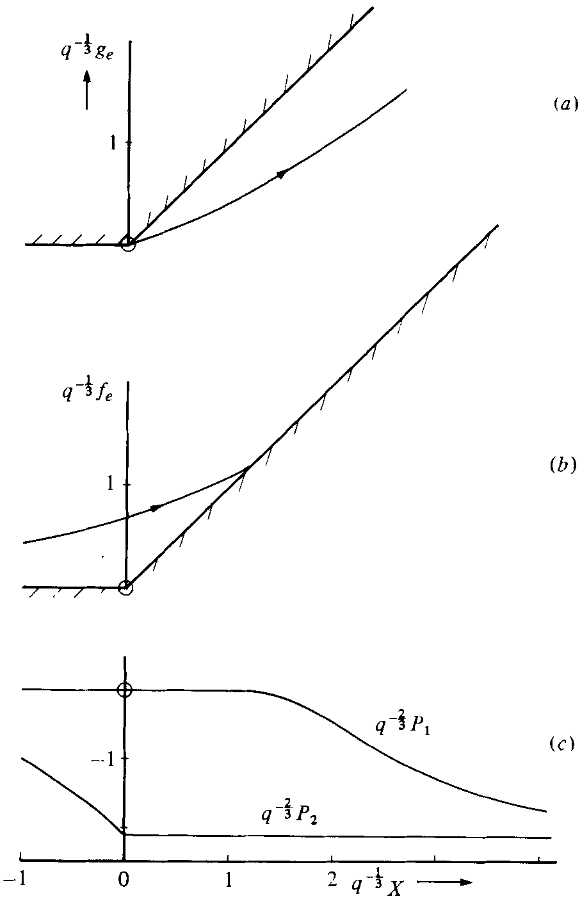

FIGURE 8. (*a*) The upper (g_e) and (*b*) the lower (f_e) free streamlines (→) versus X for the cornered channel (///). (*c*) The upper and lower wall pressures P_2, P_1.

When $0 < \alpha \ll 1$ the long scale response of § 3.1 is called into action, with l replaced by $\alpha^{-\frac{1}{3}}$ and $f(X)$, $g(X)$ both replaced by zero for $X < 0$, X for $X > 0$ (here $X = \alpha^{\frac{1}{3}}x$), leading to equation (3.6) for $A(X)$. Then for $X < 0$ the solution is given by (3.7*a*). At $X = 0$, owing to the upper corner, separation takes place at the upper wall and only *three* conditions are appropriate, namely, continuity of g_e, A and A' (analogous to those of § 3.3; g_e' is discontinuous). Between there and the reattachment at $X = X_1 > 0$ along the lower wall, the flow is detached from both walls and hence P_2 must stay constant (equal to $-C_2$, say, where C_2 is unknown) and P_1 must also (remaining zero from (3.7*a*)). So, for $0 < X < X_1$,

$$g_e(X) = -A(X) - (2C_2)^{\frac{1}{2}}, \tag{6.1a}$$

$$f_e(X) = -A(X) \tag{6.1b}$$

(only the negative square root of $2C_2$ in (6.1*a*) yields a solution of the flow problem); and, from (3.6), $qA''(X) = -C_2$, so that

$$A(X) = -\frac{C_2}{2q}X^2 + \beta X + \gamma \quad (0 < X < X_1), \tag{6.2}$$

where β, γ are unknown constants. Finally, for $X > X_1$, where the lower wall flow becomes reattached, (6.1 a) still holds but now $f_e(X) = f(X) = X$, implying (from (3.6)) the equation

$$2qA'' = (A+\alpha X)^2 - 2C_2 \tag{6.3}$$

for $A(X)$. To solve (6.3) we set $A+\alpha X = -B$. Then, with B, C_2 replacing A, C_1 respectively, $B(X)$ satisfies (3.9) and so (3.10) gives the solution. The three conditions appropriate at the reattachment point $X = X_1$ are the continuity of f_e, A and A', as in § 3.1.

Applying the first three conditions above, at $X = 0$, yields (from (6.1 a), (6.2), (3.7 a))

$$\gamma = -(2C_2)^{\frac{1}{2}}, \quad \gamma = -12q/d^2, \quad \beta = -24q/d^3, \tag{6.4}$$

respectively. The three conditions at $X = X_1$ yield, in turn,

$$X_1 = (C_2/2q)\,X_1^2 - \beta X_1 - \gamma, \tag{6.5a}$$

$$-(C_2/2q)\,X_1^2 + \beta X_1 + \gamma = (C_2/2)^{\frac{1}{2}}\,\tilde{G}_1 - X_1, \tag{6.5b}$$

$$-(C_2/q)\,X_1 + \beta = (C_2/2)^{\frac{3}{4}}\,(2-\tilde{G}_1)\,[(\tilde{G}_1+4)/3]^{\frac{1}{2}}\,q^{-\frac{1}{2}} - 1, \tag{6.5c}$$

where $\tilde{G}_1 \equiv \tilde{G}$ at $X = X_1$. Hence (6.4), (6.5 a–c) provide six equations for the determination of X_1, β, γ, C_2, $\tilde{G}_1$, d. We find the unique solution

$$d = 2[3q(1+5^{\frac{1}{2}})]^{\frac{1}{3}}, \quad X_1 = \tfrac{1}{3}(5^{\frac{1}{2}} - 2^{\frac{1}{2}})\,d, \quad \tilde{G}_1 = 0, \quad C_2 = 3(5^{\frac{1}{2}}-1)\,q/4d \tag{6.6}$$

with (6.4) then fixing β, γ.

The upper and lower free streamlines (appearing for $X > 0$ and for $X < X_1$ respectively) are depicted in figure 8. We note that the normal distance of the upper free streamline from the wall is $(2C_2)^{\frac{1}{2}}$ at $X = X_1$ and doubles to $2(2C_2)^{\frac{1}{2}}$ as $X \to \infty$. The upper and lower wall pressures, P_1, P_2, are also given in figure 8. Their ultimate approach to equality as $X \to \infty$ heralds the onset of the more conventional, boundary layer, description while governs (on the $O(Re)$ scale in x) the eventual reattachment process and the ensuing attainment of a plane attached flow description far downstream.

Finally it seems worthwhile suggesting that a further application of the features of this section is to the symmetric motion through the (severe) junction of two equal channels converging at an angle 2α at the point $(x, y) = (0, 0)$. There the cornered-channel configuration above is reflected about the outer wall ($y = \alpha x$, $x > 0$), that wall is then replaced by a line of symmetry for the flow, and the solution above (and in figure 8) describes half of the symmetrical flow field. The related problem where the fluid flow far upstream and downstream is in the direction opposite to that just considered yields a severely bifurcating symmetric channel flow, which has been studied by Bates (1978) and does not involve the upstream separation implied in the above case of the junction. We may expect, however, that the upstream separation would be involved in both unequal bifurcations and unequal junctions of channel flows and that the general approach of § 2 and above would apply then.

7. Further comments

The theory of §§ 3–6 would seem to provide a virtually complete account of the flow structure and solution properties for the classes of slowly varying severe, slender and moderately severe constriction of §§ 3, 4 and for the curved and cornered channels of §§ 5, 6, adding weight to the belief that the general structure of § 2 provides a consistent description of the high-Reynolds-number motion through a severely constricted non-symmetric channel. If the conclusions of Smith (1976*a*, *b*, 1977*a*) are also invoked, the theoretical flow features associated with almost any size of (smooth) non-symmetric constriction of the channel can now be expressed when $Re \gg 1$.

For example, let us deal first with constrictions of height comparable with the channel width but of various lengths, a^*L, supposing for argument's sake that the constriction is wedge-like (as in § 4.1) at its start. Then, if L is $O(Re)$, the flow field is described by the nonlinear boundary-layer equations throughout the channel, on the $O(a^*Re)$ streamwise length scale (Smith 1976*a*, *b*). In contrast with the flow over the constriction (where Eagles & Smith 1980 give some sample numerical solutions including separation and reattachment), the flow response upstream is only of a mild, linear, kind, taking place on the $O(a^*R^{\frac{1}{7}})$ length scale. If L lies between $O(Re)$ and $O(Re^{\frac{3}{7}})$ the upstream response is again linear (Smith 1976*b*) on the $O(a^*Re^{\frac{1}{7}})$ scale, following which the main nonlinear adjustment of the flow occurs on an $O(a^*L^{\frac{3}{2}}Re^{-\frac{1}{2}})$ streamwise scale. On that scale the constriction acts as a wedge (and § 4 of Smith 1976*a* applies), while on the longer $O(a^*L)$ scale the nonlinear adjustment (including separation) becomes inviscid and is described in effect by the properties of (4.3)–(4.4). The final adjustment phase, including reattachment and a return to the original attached motion, is governed by the $O(a^*Re)$ scale downstream. If L is reduced still further, to $O(Re^{\frac{3}{7}})$, the upstream response on the $O(a^*Re^{\frac{1}{7}})$ scale becomes nonlinear at last and upstream separation can appear (Bates 1978 gives solutions for curved and cornered channel flows when L is $O(Re^{\frac{3}{7}})$), while further downstream the $O(a^*L)$ and $O(a^*Re)$ scales operate as above. A further reduction of L forces the upstream separation of Smith (1977*a*) to arise and, indeed, if L lies between $O(Re^{\frac{3}{7}})$ and $O(1)$ then § 4.1 applies effectively. We would note however that certain stages, such as $L = O(Re^{\frac{1}{16}})$, would slightly alter the prediction of the separation position $x = x_2$ in § 4.1 (but not the overall flow structure) in view of the part played by the $O(Re^{-\frac{1}{16}})$ powers in the Sychev (1972)–Smith (1977*b*) triple-deck separation there (see (2.1) and cf. Smith 1979*b* for external flows); a similar note applies to symmetrically constricted flows also (Smith 1979*a*). Finally, when L becomes $O(1)$ the properties of § 2 are retrieved and in general a numerical solution would be required. As a second example, let us consider constrictions of various heights a^*h but whose lengths are comparable with the channel width. Then, for h of $O(1)$, the nonlinear properties of § 2 hold, while slightly reducing h brings in the nonlinear features of § 4.2 including the long scale ($O(a^*h^{-\frac{1}{2}})$) responses upstream and downstream. A further decrease of h to $O(Re^{-\frac{2}{7}})$ means that the main nonlinear responses upstream and downstream are dictated by the $O(a^*Re^{\frac{1}{7}})$ free interaction scale (on which the constriction appears as a broadside-on flat plate) and in particular the upstream separation distance in (2.3) is reduced by a significant fraction. Finally, if h is less than $O(Re^{-\frac{2}{7}})$ then the $O(a^*Re^{\frac{1}{7}})$ scale upstream effect is only linear, upstream separation is suppressed at last, and once again the work of

Smith (1976*a*, *b*) can be applied. Clearly, many other combinations of height (a^*h) and length (a^*L) scales can be fitted into the general patterns above.

For the various classes of severe constriction, cornering and curving studied in this paper we would draw attention to the surprisingly succinct nature of some of the predictions that emerge for *inter alia* separation and reattachment positions. These are given by (2.3) with (3.7*b*), table 1, (4.2), (4.5*c*), (5.3) and (6.6) for the upstream separation, by figures 3 and 4, (4.2) and (4.12) with (4.16) and (6.6) for the first reattachment point $x = x_1$, and by figures 3 and 4, (4.4) and (4.13) for the second separation point $x = x_2$. Also worthy of emphasis is the relatively complex, long-scale structure (involving core-flow perturbations of orders h and $h^{\frac{2}{3}}$) of the moderately severely constricted motion in § 4.2 compared with the straightforward structure (and only order h^2 core flow perturbations) arising in the corresponding symmetric constriction (Smith 1979*a*, § 3). The $O(h)$ and $O(h^{\frac{2}{3}})$ perturbations here are essentially eigensolutions and are associated with the nonlinear eigensolution forms of (2.5*a*–*c*) appearing upstream. Further, and perhaps equally remarkable, the first reattachment position $x = x_2$ and the contribution D to the upstream separation position (of (2.3)) can be determined, for the moderately severe case of § 4.2, only by recourse to the long scale response both upstream and downstream of the constriction, whereas the second separation point is determined by more local considerations. In all the classes studied above, and in the viscous upstream response of Smith (1977*a*) leading to (2.5*a*–*c*), a decisive part is played by the variation of the pressure across the channel due to the curvature of the core flow.

Whether or not some or all of the predicted flow features of § 3–6 may be observed experimentally or numerically in non-symmetrical channel flows is another matter. T. J. Pedley (private communication, 1979) has kindly informed us of some related experimental work in progress (at the Department of Applied Mathematics & Theoretical Physics, Cambridge) in which, for instance, there is no sign as yet of upstream separation over a significant range of Reynolds numbers, for the configuration of § 3.3; a similar phenomenon arises in smoothly, symmetrically, constricted flows (e.g. in Deshpande, Giddens & Mabon's 1976 calculations). On the other hand, Dennis & Smith's (1979) numerical flow solutions for a symmetric step-like constriction, and those of Greenspan (1969) and Friedman (1972) (see Smith 1977*a*) for non-symmetric steps, show not only the presence of upstream separation but also extraordinarily good agreement with the asymptotic theory (Smith 1977*a*, 1979*a*) as regards the upstream separation position and, in the symmetric case, the flow properties nearby. It may well be that, upstream at least (as in Smith 1979*a*), the present theory of severely constricted non-symmetric channel flows applies in practice to the more abruptly constricted flows, or to higher-Reynolds-number flows, whereas less abrupt constrictions and lower Reynolds numbers produce flows to which the earlier theories (involving only weak upstream responses: see above) are more relevant upstream (while the present theory may still apply during and beyond constriction, again as in Smith 1979*a*). More experimental and/or numerical results for the configurations considered in §§ 3–6 should help to decide the true relevance, qualitatively or quantitatively, of the present asymptotic theory at finite Reynolds numbers, however.

We are grateful to Dr T. J. Pedley for kindly pointing out the related experimental work, in progress, just referred to. One of us (F. T. S.) is grateful also to the National Sciences & Engineering Research Council of Canada for financial support, and to the Applied Mathematics Department, at U.W.O. for hospitality, during this research and to the Royal Society for a Commonwealth Travel Bursary.

REFERENCES

BATES, S. 1978 Ph.D. thesis, University of London.
COLE, J. D. & AROESTY, J. 1968 *Int. J. Heat Mass Transfer* **11**, 1167.
DENNIS, S. C. R. & SMITH, F. T. 1980 *Proc. Roy. Soc.* A (to appear).
DESHPANDE, M. D., GIDDENS, D. P. & MABON, F. R. 1976 *J. Biomech.* **9**, 165.
EAGLES, P. M. & SMITH, F. T. 1980 *J. Engng. Math.* (to appear).
FRIEDMAN, M. 1972 *J. Engng Math.* **6**, 285.
GOLDSTEIN, S. 1938 *Modern Develops in Fluid Mech.* **1**.
GOLDSTEIN, S. 1948 *Quart. J. Mech. Appl. Math.* **1**, 43.
GREENSPAN, D. 1969 *J. Engng Math.* **3**, 21.
KIRCHHOFF, G. 1869 *J. Reine angew. Math.* **70**, 289.
MESSITER, A. F. 1970 *SIAM J. Appl. Math.* **18**, 241.
MESSITER, A. F. 1979 Review in *Proc. 8th U.S. Nat. Cong. Appl. Mech.* 1978, p. 157.
PRETSCH, J. 1944 *Untersuch Mitt. dtsch. Luftfahrtf.* no. 3091.
SMITH, F. T. 1976*a* *Quart. J. Mech. Appl. Math.* **29**, 343.
SMITH, F. T. 1976*b* *Quart. J. Mech. Appl. Math.* **29**, 365.
SMITH, F. T. 1976*c* *Proc. Roy. Soc.* A **351**, 71.
SMITH, F. T. 1977*a* *J. Fluid Mech.* **79**, 631.
SMITH, F. T. 1977*b* *Proc. Roy. Soc.* A **365**, 443.
SMITH, F. T. 1979*a* *J. Fluid Mech.* **90**, 725.
SMITH, F. T. 1979*b* *J. Fluid Mech.* **92**, 171.
STEWARTSON, K. 1974 *Adv. Appl. Mech.* **14**, 145.
STEWARTSON, K. & WILLIAMS, P. G. 1969 *Proc. Roy. Soc.* A **312**, 181.
SYCHEV, V. V. 1972 *SV. Akad. Nauk. S.S.S.R., Mekh. Zh., Gaza* **3**, 47.